



TAMPERE UNIVERSITY OF TECHNOLOGY

KISHOR LAMICHHANE
SUBBAND BASED COOPERATIVE SPECTRUM SENSING
Master of Science Thesis

Examiners: Prof. Markku Renfors and Dr.
Tech. Sener Dikmese
Examiners and topic approved by: Faculty
council of Computing and Electrical Engineer-
ing on May 6, 2015

ABSTRACT

TAMPERE UNIVERSITY OF TECHNOLOGY

Master's Degree Programme in Electrical Engineering

LAMICHHANE, KISHOR: Subband based Cooperative Spectrum Sensing

Master of Science Thesis, 59 pages

October 2015

Major: Wireless Communications Circuits and Systems

Examiners: Prof. Markku Renfors and Dr. Tech. Sener Dikmese

Keywords: Cognitive radio, energy detection based cooperative spectrum sensing, subband based cooperative spectrum sensing, noise uncertainty.

Wireless communication technology with traditional rigid spectrum allocations and low scalability is wasting lots of spectral resources. Spectral congestion is becoming critical with heavily increasing utilization of wireless communications technology. Cognitive radio (CR) technology with dynamic spectrum management capabilities is widely advocated for utilizing effectively the unused spectrum resources. The main idea behind CR technology is to trigger secondary communications to utilize the unused spectral resources. However, CR technology heavily relies on spectrum sensing techniques which are applied to estimate the presence of primary user (PU) signals.

The studies of this thesis focus on energy detection (ED) based semi-blind sensing schemes. ED based sensing only requires the knowledge of noise variance, which can be obtained according to the previous noise measurements. To counteract the practical wireless channel effects, collaborative approach of PU signal estimation i.e., cooperative spectrum sensing (CSS) techniques are investigated. CSS eliminates the problems of both hidden nodes and fading multipath channels. Additionally, subband based CSS scheme will be developed. Fast Fourier transform (FFT) and analysis filter bank (AFB) based receiver side processing methods are used. Subband energies are then processed for ED based CSS methods. The studies show that filter bank based multicarrier (FBMC) waveform with better spectral containment improves the performance significantly. Additionally, cooperative maximum-minimum energy detection (Max-Min ED) method is proposed. The proposed method is immune to the noise uncertainty effects, which is a critical issue in traditional ED based spectrum sensing. Cooperative maximum-minimum energy detection (Max-Min ED) shows better spectrum sensing performance compared with traditional CSS schemes under noise uncertainty conditions.

Overall, the thesis contributes to better understanding and handling of subband based CSS in CR system. The proposed novel cooperative Max-Min ED greatly reduces the complexity compared to existing techniques which are robust to the noise uncertainty effects. These contributions are expected to provide a useful tool for the design and implementation of flexible, efficient, and simple spectrum sensing mechanism for CR technology.

PREFACE

This Master of Science thesis has been written for the completion of Master of Science (Technology) in Electrical Engineering from Tampere University of Technology (TUT), Tampere Finland. The research leading to this thesis has been carried out in the Department of Communications Engineering.

First and foremost, I am pleased to express my gratitude to my supervisor Professor Dr. Tech. Markku Renfors for examining and guiding me throughout the thesis. It has been a privilege to have the opportunity to study under his guidance.

I would also like to thank Dr. Tech. Sener Dikmese for his continuous support throughout these studies. Thank you for always being ready to help with all the problems that I came up with. His way of sharing knowledge and willing to help attitude has always supported me a lot to foster these studies in correct direction.

Finally, it is a pleasure to express my gratitude towards family and friend for their continuous support and motivation to pursue this Master's degree.

Tampere, October 2015

Kishor Lamichhane

CONTENTS

Abstract	i
Preface	ii
Table of Contents	iv
Terms and Definitions	v
List of Symbols	vii
List of Figures	xi
1. Introduction	1
1.1 Background and Motivation	1
1.2 Objectives and Scope of the Thesis	3
1.3 Outline of the Thesis	3
2. Cognitive Radio and Traditional Spectrum Sensing	4
2.1 Cognitive Radio	4
2.2 Spectrum Sensing Methods for Cognitive Radio	5
2.2.1 Energy Detection based Spectrum Sensing	9
2.2.2 Eigenvalue based Sensing	11
2.2.3 Other Sensing Methods	12
2.2.4 Cooperative Spectrum Sensing	12
2.3 System Model	12
2.3.1 PU Signal Models	12
2.3.2 Channel Model and Pathloss	13
3. Traditional Cooperative Spectrum Sensing	14
3.1 Introduction	14
3.2 Cooperative Strategies	16
3.3 Hard Decision Fusion with Linear Fusion Rules	16
3.3.1 OR Rule	17
3.3.2 AND Rule	17
3.3.3 Majority-Rule	17
3.3.4 Generalized Rule of k-out-of-M	18
3.3.5 Optimized k-out-of-M Rule	18
3.4 Traditional CSS Algorithms	19
3.5 Simulation Results	20
3.5.1 Log-Normal Pathloss with AWGN	20
3.5.2 Frequency Selective Channel	24
3.6 Chapter Summary	27
4. Proposed FFT and AFB based Cooperative Spectrum Sensing	28
4.1 Introduction	28
4.1.1 FFT and AFB Basics	30

4.1.2	Multicarrier Systems	31
4.2	FFT and AFB based Energy Detector Algorithms	31
4.3	FFT/AFB based cooperative spectrum sensing	33
4.4	Simulation Results	34
4.5	Chapter Summary	36
5.	Maximum-Minimum subband energy based Cooperative Spectrum Sensing . . .	37
5.1	Introduction	37
5.2	Proposed Max-Min ED based CSS Method	38
5.2.1	Subband Energy Detector	39
5.2.2	Cooperative Maximum-Minimum Energy Detection	39
5.3	Analytical Models for Max-Min based Energy Detector	40
5.3.1	Probability of False Alarm and Energy Threshold	40
5.3.2	Probability of Detection	41
5.3.3	Analysis of Cooperative Maximum-Minimum Energy Detection . . .	42
5.4	Simulation Results	42
5.4.1	Comparison of Max-Min ED, Max/Min ED, and differential Max-Min ED based CSS	43
5.4.2	Comparison of Analytical and Simulated Results of Max-Min ED and Traditional Cooperative ED	46
5.5	Chapter Summary	52
6.	Conclusion	54
	References	55

TERMS AND DEFINITIONS

ADC analog-to-digital converter

AFB analysis filter bank

AWGN additive white Gaussian noise

CMT cosine modulated multitone

CP-OFDM cyclic prefix based orthogonal frequency division multiplexing

CSI channel state information

CSS cooperative spectrum sensing

CR cognitive radio

DFT discrete Fourier transform

DWMT discrete wavelet multitone

ED energy detection

ESD energy spectral density

FBMC filter bank based multicarrier

FC fusion center

FCC Federal Communications Commission

FDM frequency-division multiplexing

FFT fast Fourier transform

FMT filtered multitone

IFFT inverse fast Fourier transform

ITU International Telecommunication Union

Max-Min ED maximum-minimum energy detection

OFDM orthogonal frequency division multiplexing

PSD power spectral density

PU primary user

QAM quadrature amplitude modulation

QPSK quadrature phase shift keying

ROC receiver operating characteristics

SDR software defined radio

SED subband energy detector

SFB synthesis filter bank

SNR signal to noise ratio

SU secondary user

SUI Stanford University interim

WLAN wireless local area network

LIST OF SYMBOLS

This is a list of the principle symbols and notations used throughout the thesis

A_c	Carrier amplitude
\mathcal{H}_0	Hypothesis 0 in Neyman-Pearson test
\mathcal{H}_1	Hypothesis 1 in Neyman-Pearson test
$h[n]$	Channel's impulse response
c_f	Carrier frequency
k_f	Frequency sensitivity
\mathcal{Q}_G	Gumbel distribution
L_f	Length of frequency averaging window
M	Number of sensing station
$m(t)$	Voice signal
N	Observation length
N_{FFT}	Number of FFT points
\mathcal{N}	Obeying Gaussian distribution
P_D	Detection probability
P_{FA}	False alarm probability
$P_{D,t}$	Cooperative detection probability
$P_{FA,t}$	Cooperative false alarm probability
$P_r(\cdot \cdot)$	Contingent probability
$Q(\cdot)$	Gaussian Q-function
$Q^{-1}(\cdot)$	Inverse Gaussian Q-function
$s[n]$	Generated wireless microphone signal
$s(t)$	Generated FM signal
$T(y)$	Test Statistics
$w[n]$	AWGN samples
$x[n]$	Transmitted signal
$y[n]$	Observed complex signal
σ_n^2	Noise variance
σ_x^2	Signal variance
λ	Threshold value
γ	SNR value

LIST OF FIGURES

2.1	Various aspects of spectrum sensing for cognitive radio [6]	6
2.2	Spectrum sensing techniques [15]	8
2.3	Traditional ED based spectrum sensing for QPSK signal with AWGN channel and $N = 1000$	10
3.1	CR topology including PU signals and M CR users	15
3.2	Block diagram of traditional cooperative spectrum sensing techniques . .	19
3.3	CSS detection probabilities against SNR with basic ED and three different linear fusion rules for a channel with frequency-flat log-normal fading with 6 dB standard deviation. The sample complexity is $N = 10240$, the number of sensing stations $M = 8$, $P_{FA} = 0.01$ for each station. a) QPSK, b) 16-QAM and c) 64-QAM.	21
3.4	ROC curve at $\gamma = -15$ dB with basic ED and three different linear fusion rules for a channel with frequency-flat log-normal fading with 6 dB standard deviation. PU signal model is 16-QAM, the sample complexity is $N = 10240$, the number of sensing stations $M = 8$	22
3.5	CSS detection probabilities against SNR with basic ED and three different linear fusion rules for a channel with frequency-flat log-normal fading with 9 dB standard deviation. PU signal model is 16-QAM, the sample complexity is $N=10240$, the number of sensing stations $M=8$, and $P_{FA} = 0.01$ for each station.	23
3.6	ROC curve at $\gamma = -13$ dB with basic ED and three different linear fusion rules for a channel with frequency-flat log-normal fading with 9 dB standard deviation. PU signal model is 16-QAM, the sample complexity is $N = 10240$, and the number of sensing stations $M = 8$	23
3.7	CSS detection probabilities with basic ED and three different linear fusion rules for frequency-flat log-normal fading with standard deviation 9 dB. PU signal model is 64-QAM, the sample complexity $N = 10240$, the number of sensing stations $M = 8$, and $P_{FA} = 0.01$ for each sensing station. a) Indoor channel, b) ITU-R vehicular A channel, and c) SUI-I channel.	24
3.8	ROC curve at $\gamma = -14$ dB with basic ED and three different linear fusion rules for the Indoor channel with frequency-flat log-normal fading with standard deviation 9 dB. PU signal model is 64-QAM, the sample complexity $N = 10240$, and the number of sensing stations $M = 8$	25

3.9	ROC curve at $\gamma = -13$ dB with basic ED and four different linear fusion rules for the ITU-R vehicular A channel with frequency-flat log-normal fading with standard deviation 9 dB. PU signal model is 64-QAM, the sample complexity $N = 10240$, and the number of sensing stations $M = 8$.	26
3.10	ROC curve at $\gamma = -12$ dB with basic ED and three different linear fusion rules for the SUI-1 channel with frequency-flat log-normal fading with standard deviation 9 dB. PU signal model is 64-QAM, the sample complexity $N = 10240$, and the number of sensing stations $M = 8$.	27
4.1	System model for spectrum sharing in CR.	29
4.2	Interference model between primary and secondary users	30
4.3	Effects of the power amplifier model on (a) OFDM and (b) FBMC based primary user (PU)s spectra.	30
4.4	Block diagram of alternative filter bank (AFB) and fast Fourier transform (FFT) based spectrum analysis methods for subband energy based cooperative sensing schemes.	31
4.5	Block diagram of fast Fourier transform (FFT) and analysis filter bank (AFB) based cooperative spectrum technique.	33
4.6	Comparison of CSS false alarm probabilities between FFT processing of OFDM based PU and AFB processing of FBMC based PU with three different linear fusion rules under ideal mode (no PA effects) for $N_{FFT} = 250$, the time record length $N_t = 50$, the frequency block length $N_f = 5$, and the number of sensing stations $M = 8$.	34
4.7	Comparison of CSS false alarm probabilities between FFT processing of OFDM based PU and AFB processing of FBMC based PU with three different linear fusion rules under power amplifier effects for $N_{FFT} = 250$, the time record length $N_t = 50$, the frequency block length $N_f = 5$, and the number of sensing stations $M = 8$.	35
4.8	CSS false alarm probabilities for FFT processing of a) OFDM and b) FBMC based PU with three different linear fusion rules under power amplifier effects for the number of FFT length is $N_{FFT} = 250$, the time record length $N_t = 50$, the frequency block length $N_f = 5$, and the number of sensing stations $M = 8$.	36
5.1	Block diagram of Max-Min ED based CSS method.	38
5.2	CSS detection probabilities with a) Max-Min ED, b) Max/Min ED and c) Diff. Max-Min ED and three different linear fusion rules for non-oversampled QPSK PU signal under Indoor channel, the length of fast Fourier transform (FFT) $N_{FFT} = 8$, the number of sensing stations $M = 8$, the sample complexity $N = 10240$, and 1 dB noise uncertainty.	43

5.3 CSS detection probabilities with a) Max-Min ED, b) Max/Min ED and c) Diff. Max-Min ED and three different linear fusion rules for small-oversampled QPSK PU signal under Indoor channel, the length of FFT $N_{FFT} = 8$, number of sensing stations $M = 8$, the sample complexity $N = 10240$, and 1 dB noise uncertainty 44

5.4 CSS detection probabilities with a) Max-Min ED, b) Max/Min ED and c) Diff. Max-Min ED and three different linear fusion rules for 2x-oversampled QPSK PU signal under Indoor channel, the length of FFT $N_{FFT} = 8$, number of sensing stations $M = 8$, the sample complexity $N = 10240$, and 1 dB noise uncertainty. 45

5.5 CSS detection probabilities with a) Max-Min ED, b) Max/Min ED and c) Diff. Max-Min ED and three different linear fusion rules for 2x-oversampled QPSK PU signal under Indoor channel, the length of FFT $N_{FFT} = 32$, the number of sensing stations $M = 8$, the sample complexity $N = 10240$, and 1 dB noise uncertainty. 46

5.6 Comparison of CSS detection probabilities between traditional ED and Max-Min ED with three different linear fusion rules for 2x-oversampled QPSK PU signal under Indoor channel model, the length of FFT $N_{FFT} = 8$, the number of sensing stations $M = 8$, the sample complexity $N = 10240$, and 1 dB noise uncertainty. 47

5.7 Comparison of detection probabilities between traditional ED and Max-Min ED with three different linear fusion rules for 2x-oversampled QPSK PU signal under Indoor channel model, the length of FFT $N_{FFT} = 32$, the number of sensing stations $M = 8$, and the number of sampling complexity $N = 10240$, and 1 dB noise uncertainty. 48

5.8 Comparison of CSS ROC curve with both basic ED and Max-Min ED and three different fusion rules at $\gamma = -14$ dB for 2x-oversampled PU signal without frequency selective channel and fading effects, the number of sensing stations $M = 8$, the length of FFT $N_{FFT} = 8$, and the sample complexity $N = 10240$ 49

5.9 Comparison of CSS ROC curve with both basic ED and Max-Min ED and three different fusion rules at $\gamma = -14$ dB for 2x-oversampled PU signal without frequency selective channel and fading effects, the number of sensing stations $M = 8$, the length of FFT $N_{FFT} = 8$, the sample complexity $N = 10240$, and 0.1 dB noise uncertainty. 50

- 5.10 Comparison of CSS ROC curve with both basic ED and Max-Min ED and three different fusion rules at $\gamma = -14$ dB for 2x-oversampled PU signal, the channel model is SUI-I with frequency flat lognormal fading with standard deviation 9 dB, the number of sensing stations $M = 8$, the length of FFT $N_{FFT} = 8$, the sample complexity $N = 10240$, and noise uncertainty parameter [0,1] dB. 51
- 5.11 Comparison of CSS ROC curve with both basic ED and Max-Min ED and three different fusion rules at $\gamma = -14$ dB for 2x-oversampled PU signal, the channel model is SUI-I with frequency flat lognormal fading with standard deviation 9 dB, the number of sensing stations $M = 8$, the length of FFT $N_{FFT} = 8$, the sample complexity $N = 10240$, and 0.1 dB noise uncertainty. 52

1. INTRODUCTION

1.1 Background and Motivation

With the growing attention in wireless communication, spectral scarcity is becoming modern days' challenge. Higher demand of spectral bandwidth is pushing spectrum usage to utmost limits. However, the limitations of traditional wireless technology leads to lots of spectrum wastage, inviting opportunistic usages of those rare unused resources [1]. These studies mainly focused on technologies that solve the problem of spectral scarcity by using opportunistically the frequency band to establish secondary communication. Such technology is commonly known as cognitive radio (CR). CR technology defines new dimension to the modern communication system advocating environment adaptive radio transmission [2]. CR keeps track of the radio transmission environment continuously while it dynamically varies its transmission parameters so as to adjust its operation to the surroundings. Hence, managing of the secondary communication to the utmost perfection depends on the following three CR functions:

- Radio-scene analysis,
- Estimation of channel state information (CSI) including predictive modeling,
- Transmit-power control and dynamic spectrum management.

Radio-scene analysis has two functions of estimating interference temperature and detection of spectral holes. Spectral holes are the band of frequencies assigned to a primary user, but, at a particular time and specific geographic location, the band is not being utilized by that user. CSI estimation and predictive modeling is another step, where CSI is estimated using either differential techniques or via the pilot transmission. Third and the final step is the transmit-power control and the dynamic spectrum management that controls the transmit power within each frequency slot of the used frequency band in order to manage spectrum dynamically. Here the power control mechanism is either cooperative or non-cooperative [3] [4]. However, the most important step among the three is radio resource analysis, as CR technology heavily relies on the results of radio scene analysis. As PU is solely authorized to spectrum usage, radio scene analysis is considered as a gateway to the secondary communication. Hence, secondary communication heavily relies on the number of spectral holes [3]-[6]. The matter of primary interest is that spectrum sensing

predicts precisely the available holes so as to trigger secondary communication [7]. Our studies mainly focused on the radio scene analysis i.e., spectrum sensing.

Spectrum sensing based CR technology is considered as highly interesting topic in wireless communications. Spectrum sensing, in other words, involves tracking of the PU activity so as to estimate the spectral holes. Different sensing algorithms find the availability of spectral holes as an opportunity to enable the secondary communication. Recent studies have suggested a wide variety of spectrum sensing techniques, but none of them is fully satisfying in terms of all relevant metrics like implementation complexity, reliability, and loss in secondary system throughput. Especially, spectrum sensing under low signal to noise ratio (SNR) is widely covered in the literature, under conditions where the noise dominates the weak PU signal. Under these conditions, the spectrum sensing becomes very critical to imperfect knowledge of the power and characteristics of the noise [8] [9] [10].

Spectrum that is originally assigned to the PU can be used by secondary user (SU) if and only if PU becomes idle. Since SUs can only use spectrum as an opportunity, spectrum sensing has a great role to play in CR technology. Regarding the importance of the radio scene analysis function, basic spectrum sensing methods show numerous limitations. Shadowing, hidden node problems, etc., always make spectrum sensing challenging. A PU transmission may be unobservable for a CR sensing station while its signal is fully usable by a nearby PU receiver. In order to make the spectrum sensing function reliable, efficient, and to counteract both multipath and hidden node problems, cooperative spectrum sensing (CSS) comes into the light. CSS involves two or more cooperative radio receivers in decision making during spectrum sensing. Recent research [11] [12] suggests possibility of collaboration among number of CR users to enhance the detection performance. Our studies further exploiting the collaborative approach of spectrum sensing commonly termed as CSS. The studies of this thesis mainly focus on those spectrum sensing methods that add the collaboration among a number of CR receivers to enhance the detection performance and to counteract practical wireless channel effects. CSS exploits the diversity among a number of CR receivers having different multipath channel profiles and experience different large-scale fading (shadowing) characteristics towards the PU transmissions [13] [14].

Additionally, the studies in this thesis considers the novel Max-Min ED based CSS. Specifically, this thesis extends the earlier studies of our group on Max-Min ED [15] [16] to cooperative spectrum sensing. The proposed novel method is expected to effectively overcome the issue of noise uncertainty with remarkably lower implementation complexity compared to existing methods. For the subband decomposition, both FFT and analysis filter bank (AFB) techniques are considered and the resulting performance is compared. The developed algorithm with reduced complexity, enhanced detection performance, and improved reliability is presented as an attractive solution to counteract the practical wire-

less channel effects under low SNR [17] [18].

1.2 Objectives and Scope of the Thesis

The objective of the studies is first to analyze the existing spectrum sensing techniques. Then novel sensing schemes are proposed to solve practical challenges. The studies mainly focus on cooperative sensing techniques. Hard decision based fusion rules, such as "AND rule", "OR rule" and "Majority rule", are implemented to exploit collaboration among CR users. Our studies do not cover soft decision based CSS, which remains as an important topic for future work. Additionally, an effective subband based spectrum sensing method is elaborated for the CSS application. MATLAB based simulation model is developed for validating and evaluating the performance of the developed methods.

1.3 Outline of the Thesis

The thesis is organized into six chapters. It introduces the CR technology and its spectrum sensing techniques. The study in this thesis is focused on the energy detection (ED) based schemes, which are semi-blind methods. They need no prior PU information other than noise variance. The main focus is on collaborative approach among a number of SUs and termed as CSS. The thesis proposes subband based CSS approach as a novel scheme to solve issues introduced by practical wireless channel effects.

The Structure of the thesis is as follows:

- Chapter 2 covers the CR technology and its functions. Additionally, the chapter introduces spectrum sensing algorithms. Specifically, the chapter converges on ED based techniques.
- Chapter 3 covers the traditional collaborative approach to counteract the practical wireless channel effects. The chapter converges to cooperative strategies based on ED based spectrum sensing techniques. Additionally, the chapter includes simulation results for basic CSS schemes which are analyzed accordingly.
- Chapter 4 covers the subband based spectrum sensing techniques. The chapter proposes novel FFT and AFB based cooperative sensing techniques. The chapter also includes the simulation results and analysis of the proposed solution.
- Chapter 5 proposes a novel maximum-minimum ED based CSS. The novel scheme reduces complexity and is robust to the noise uncertainty. Additionally, the chapter includes simulation results and analysis of the proposed scheme.
- The final chapter summarizes the results and learning of this work.

2. COGNITIVE RADIO AND TRADITIONAL SPECTRUM SENSING

In this chapter, CR and its functions are discussed. Recalling the literature on CR technology, the studies are mainly centered on its radio scene analysis function i.e., spectrum sensing techniques. Chapter considers three different functions of CR technology. After completion of this chapter we aim to learn the following aspects:

- CR and different functions of CR technology.
- Radio scene analysis function and its importance in CR technology.
- Various spectrum sensing techniques with their advantages and drawbacks. The methods are classified to blind, semi-blind and non-blind spectrum sensing techniques.
- Working principle of ED based semi-blind techniques and subband based methods.

This chapter covers the CR and spectrum sensing techniques in general. Section 2.1 is an outline of CR technology and covers its evolution, advantages, and main functions. Section 2.2 gives the description of selected important spectrum methods, with emphasis on ED based techniques. Section 2.3 presents the system model for spectrum sensing studies, including the PU signal model and channel models.

2.1 Cognitive Radio

With increasing spectral congestion of the radio spectrum, CR is now emerging as a promising solution. According to the Federal Communications Commission (FCC) only a few portions of the spectrum is being utilized effectively whereas the rest of the precious spectrum is partially wasted [1]. According to the research reports [2] [5] some frequency bands in the spectrum are largely unoccupied most of the time while some others are only partially occupied and the rest are heavily used. The under utilization of the spectrum leads us to think in terms of spectral holes which can be defined as bands of frequencies assigned to a primary user, but, at a particular time and specific geographic location, the band is not being utilized by that user [4]. CR technology is now emerging as a solution to utilize that band which is mostly underutilized by licensed users. CR can automatically detect available channels in the wireless spectrum so as to use the best wireless

channels in its vicinity. Hence CR can accordingly change its transmission parameters by estimating its current wireless channel conditions to manage more efficiently concurrent wireless communications in a given spectrum band and location [6]. CR technology involves three steps: The first one is radio-scene analysis which involves determination of spectral holes, i.e., spectrum sensing. The second one is the channel identification which involves the both CSI estimation and identification of channel capacity. The third and the last step is the controlling of transmit power in different slots of the used frequency band [3]. CR applies the concept of unused bandwidth utilization only when the licensed PU is in idle mode [4]. CR is based on the concept of software defined radio (SDR) architecture, which provides the possibility to adjust the radio parameters in real time with the aid of radio scene analysis and transmit power control [4][20].

SU is allowed to utilize spectrum when PU is in idle mode. Spectrum sensing becomes critical to determine the availability of particular spectrum. In other words, spectrum sensing has pivotal role on CR network to ensure the good secondary communication for SU usage. The reliability of CR networks highly depends on spectrum sensing accuracy, irrespective of the CR network architecture. With shadowing, hidden node problem and multipath effects, a single CR receiver cannot predict reliably the actual spectrum availability. To mitigate those effects, the concept of collaborative approach i.e., CSS has evolved. CSS introduces the cooperation among two or more CR receivers to determine the availability of PU spectrum [4] [15] [16].

2.2 Spectrum Sensing Methods for Cognitive Radio

Identification of the underutilized spectrum is the main task of the spectrum sensing function. In sensing based CR system, secondary communication solely depends on the spectrum sensing function of CR technology. As channel conditions vary continuously, regular monitoring is required for effective CR operation, including cooperation with other users [4][15][16]. Frequency spectrum can be categorized into three different types according to the activity on subbands: white space band, grey space band, and black space band [19]. White space band refers to the band which is free and only contains noise. Grey space band refers to the band with partial or uncertain occupancy. Black space band refers to the band that is fully occupied. Spectrum sensing determines both the white space band and grey space band to check the availability of the spectrum.

Various steps and challenges that are involved in spectrum sensing have been portrayed in Figure 2.1. Challenges and the enabling algorithms of the spectrum sensing techniques are covered in this figure. Additionally, the figure includes both the standards that employ the spectrum sensing and the sensing approaches. Challenges have been classified as follows:

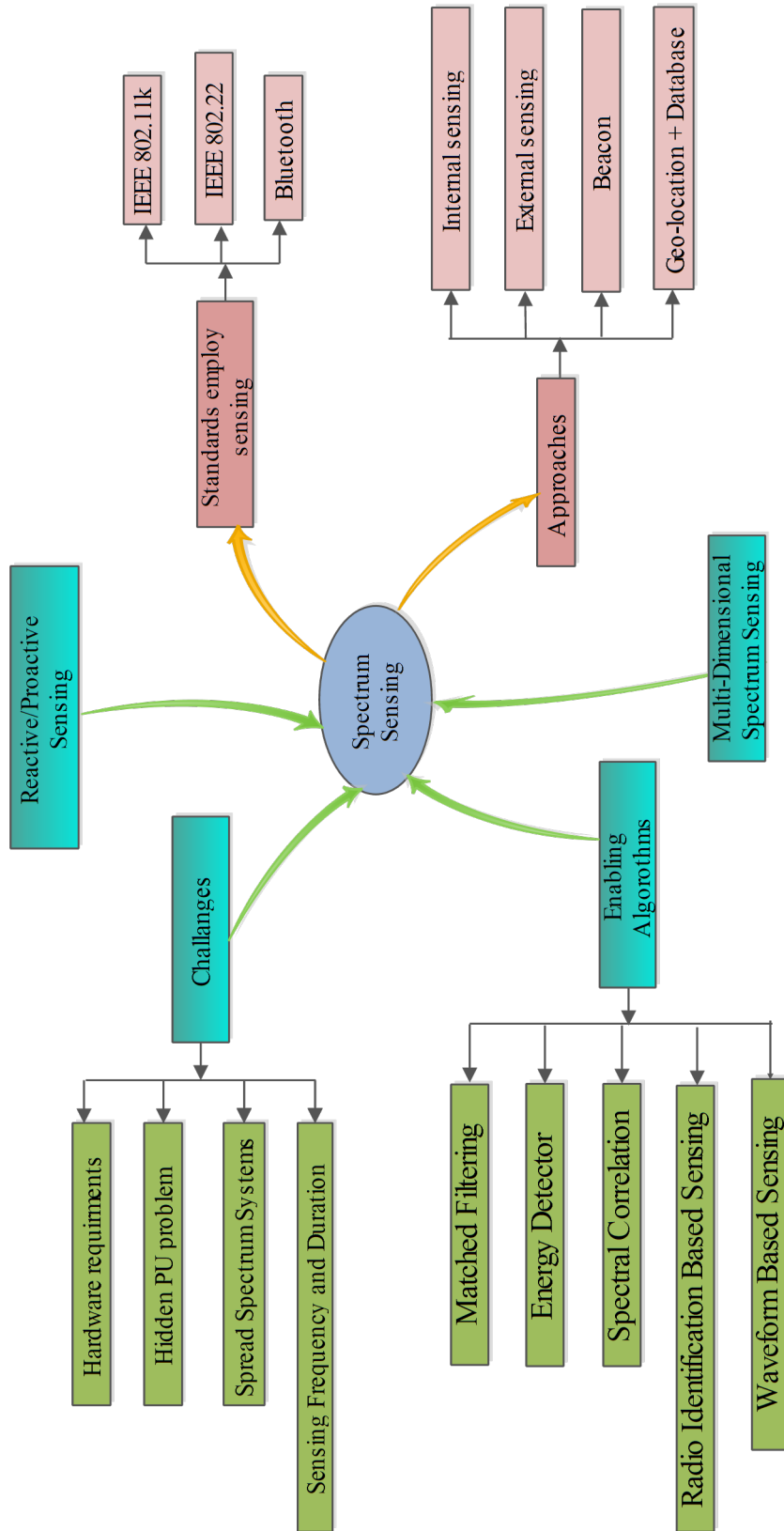


Figure 2.1: Various aspects of spectrum sensing for cognitive radio [6]

Challenges:

- hardware requirements,
- hidden PU problem,
- spread spectrum systems, and
- sensing frequency and duration.

Figure also portrays the enabling algorithms and further classified into as follows:

Enabling algorithms:

- matched filtering,
- ED,
- spectral correlation,
- radio identification based sensing, and
- waveform based sensing.

Since spectrum sensing is one of the critical functions in CR technology, it needs to be efficient and effective. Time- and frequency-domain as well as space-domain sensing techniques are in current practice. Spectrum sensing has to address the practical wireless channel effects. In practical scenarios, signals are expected to be at very low SNR level and the mobile channel also adds the challenges like frequency selectivity and temporal variations of the signal strength i.e., fading. Regarding the implementation and reliability, spectrum sensing techniques have to be simple and accurate.

Figure 2.2 depicts different methods of spectrum sensing. These sensing techniques are categorized into blind, semi-blind and non-blind technique [6][16]. Blind techniques does not require any knowledge of the PU signals. Both eigenvalue and co-variance based methods are examples of blind spectrum sensing methods. Non-blind techniques require prior PU information, which is generally not available in typical spectrum sensing scenarios, and are complex to implement. Semi-blind techniques require limited information about the observed signal, like noise variance or some general PU characteristics. ED is one of the commonly used semi-blind methods that predicts the availability of spectrum with the help of noise variance and needs no other PU information. ED based sensing algorithms will be described with details in a following section. The studies are mainly focused on ED based semi-blind sensing techniques. The studies in this thesis are extended to cover the Max-Min ED based blind spectrum sensing techniques [4] [6] [15] [16].

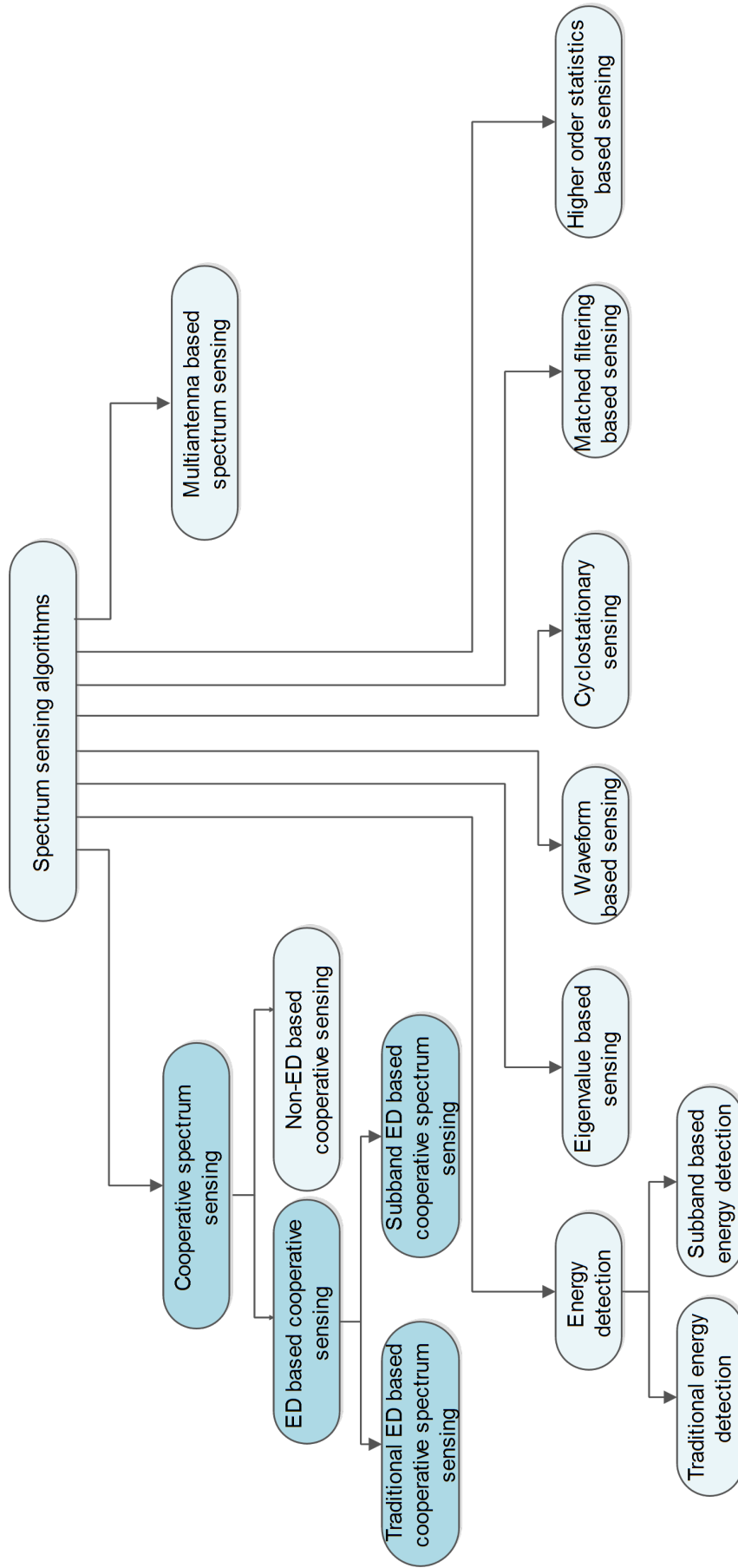


Figure 2.2: Spectrum sensing techniques [15]

2.2.1 Energy Detection based Spectrum Sensing

ED is one of the most commonly used spectrum sensing techniques. In addition to the traditional basic ED, various subband energy based schemes have been developed recently. Subband based techniques involve division of the observed signal into a number of subbands to investigate spectrum availability with better frequency resolution and to utilize information about the power spectrum variability for sensing purposes [4] [6].

Traditional Energy Detector

Traditionally, ED based sensing technique is one of the easiest forms to sense the spectrum. It uses signal energy to decide whether the spectrum is free or occupied by the PU. There is one case where no PU signal is present, i.e., the observed signal consists only of noise, and this is formulated as '*absent hypothesis*', \mathcal{H}_0 . The other case where signal and noise both present and hence formulated as '*present hypothesis*', \mathcal{H}_1 .

When a primary signal, $x(t)$, is transmitted through a wireless channel with channel gain h , the observed signal at the receiver, $y(t)$, which follows a binary hypothesis model, can be given as:

$$y(t) = \begin{cases} w(t) & \mathcal{H}_0 \\ hx(t) + w(t) & \mathcal{H}_1 \end{cases} \quad (2.1)$$

where $w(t)$ is the additive white Gaussian noise (AWGN). Complex basedband system model is assumed, i.e., $x(t)$, $y(t)$ and $w(t)$ are complex. The corresponding test statistics can be obtained as $T(y) = 1/N \sum_{n=0}^{N-1} |y[n]|^2$, where N represents observation sequence length. With relatively high values of N , as commonly required in the spectrum sensing applications, the probability distribution of the ED test statistics can be well approximated by the Gaussian distribution, both under \mathcal{H}_0 and \mathcal{H}_1 . This can be formally expressed as follows:

$$T(y)|_{\mathcal{H}_0} \sim \mathcal{N}\left(\sigma_w^2, \frac{\sigma_w^4}{N}\right) \quad (2.2)$$

and,

$$T(y)|_{\mathcal{H}_1} \sim \mathcal{N}\left(\sigma_x^2 + \sigma_w^2, \frac{(\sigma_x^2 + \sigma_w^2)^2}{N}\right), \quad (2.3)$$

where σ_w^2 and σ_x^2 are the noise and signal variance, respectively.

The probability of false alarm (P_{FA}) is calculated under \mathcal{H}_0 hypothesis and detection probability P_D is calculated under \mathcal{H}_1 hypothesis where the signal and noise is both present. P_{FA} and P_D are probabilities of getting test statistics T above predefined threshold λ .

$$P_{FA} = P_r(T(y) > \lambda |_{\mathcal{H}_0}) = Q\left(\frac{(\lambda - \sigma_w^2)}{\sigma_w^2 / \sqrt{N}}\right) \quad (2.4)$$

$$P_D = P_r(T(y) > \lambda | \mathcal{H}_1) = Q \left(\frac{(\lambda - \sigma_w^2(1 + \gamma))}{\sigma_w^2(1 + \gamma)/\sqrt{N}} \right), \quad (2.5)$$

where $Q(\cdot)$ is the Gaussian Q function, γ represents the SNR level and λ is the threshold value. The probability of detection depends on the value of predefined threshold which is commonly set to reach the target false alarm probability. Consequently, the detection probability is a function of SNR and P_{FA} [9] [10] [15] [16].

With noise uncertainty, both detection and false alarm probabilities vary. Detection and false alarm probabilities under noise uncertainty condition can be represented as follows:

$$P_D = P_r(T(y) > \lambda | \mathcal{H}_1) = Q \left(\frac{(\lambda - \sigma_w^2((1/\rho) + \gamma))}{\sigma_w^2((1/\rho) + \gamma)/\sqrt{N}} \right), \quad (2.6)$$

$$P_{FA} = P_r(T(y) > \lambda | \mathcal{H}_0) = Q \left(\frac{(\lambda - \rho\sigma_w^2)}{\rho\sigma_w^2/\sqrt{N}} \right) \quad (2.7)$$

where, ρ is a noise uncertainty parameter and is equal to $10^{NU_{dB}/10}$. NU_{dB} is noise uncertainty in dB scale.

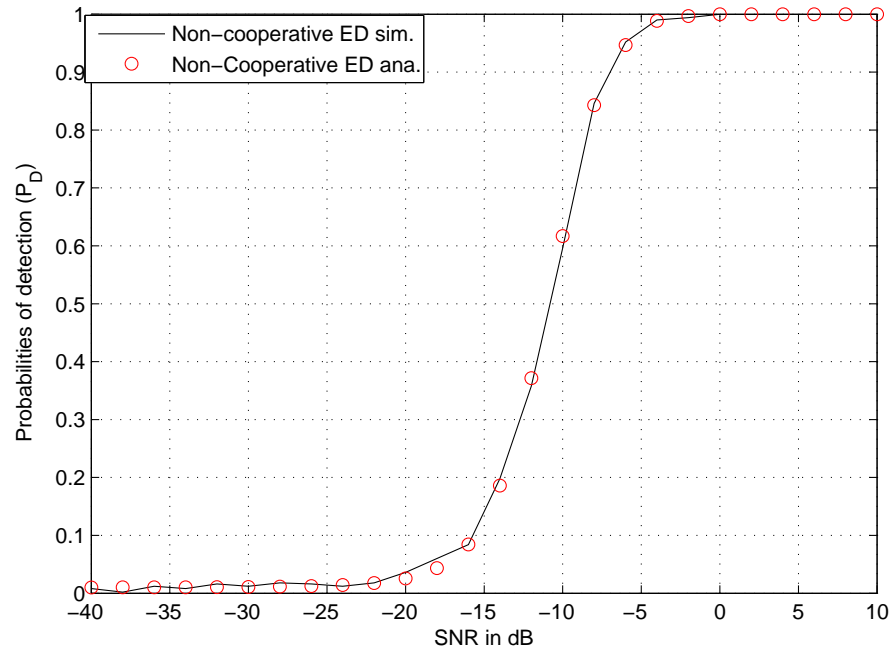


Figure 2.3: Traditional ED based spectrum sensing for QPSK signal with AWGN channel and $N = 1000$.

Figure 2.3 shows a comparison of theoretical and simulated performance of ED for AWGN channel as a function of SNR for $P_{FA} = 0.01$. Close match of the simulated and theoretical performance can be observed.

Subband Energy Detector

Subband based ED methods have been used for the spectrum analysis of wideband signals. Such approaches help to identify spectral holes rapidly and allocate the most feasible part of the bands for CR operation. In this thesis, FFT and AFB have been implemented as main techniques to process spectrum into a number of subbands. Block-wise FFT processing is one of the most commonly used approaches which measures the power in each subband for further processing. However, FFT has serious limitations in this task due to effects of spectrum leakage. AFB based method is the alternative subband based approach found to be particularly interesting for CR communications [15] [17]. Specifically, AFB is found to be beneficial in high-dynamic range scenarios when performing the sensing in the presence of strong transmissions at nearby frequencies. In subband based ED approach, the subband signal $Y_k[m]$ can be represented as follows:

$$Y_k[m] = \begin{cases} \mathcal{W}_k[m] & \mathcal{H}_0 \\ S_k[m]H_k + \mathcal{W}_k[m] & \mathcal{H}_1 \end{cases} \quad (2.8)$$

where $S_k[m]$ is the transmitted signal by PU as it appears at the m^{th} FFT or AFB output sample in subband k , and $\mathcal{W}_k[m]$ is the corresponding channel noise sample. As earlier, \mathcal{H}_0 and \mathcal{H}_1 denote the absent and present hypothesis of the PU signal, respectively. When the AWGN only is present, the white noise is modeled as a zero-mean Gaussian random variable with variance σ_w^2 i.e., $\mathcal{W}_k[m] = \mathcal{N}(0, \sigma_w^2)$. In many cases, the PU signal can also be modeled as a zero-mean Gaussian variable $S_k[m] = \mathcal{N}(0, \sigma_k^2)$ where, σ_k^2 is the variance (power) at subband k . FFT or AFB based approach is one of the emerging subband based approaches and is particularly interesting when orthogonal frequency division multiplexing (OFDM) or filter bank based multicarrier (FBMC) waveform is used for secondary transmission [15] [17][31]. FFT and AFB based CSS is the main topic of this study and will be explained in details in Chapter 4.

2.2.2 Eigenvalue based Sensing

Eigenvalue based sensing is one of the sensing techniques, which does not require knowledge of noise variance in the observation. It can be regarded as a potential solution to the noise uncertainty issue. As noise variance has no use in the eigenvalue and covariance based spectrum sensing methods, changes or uncertainty of noise variance have minor effect on sensing performance. However, eigenvalue based techniques have the drawback of high implementation complexity. In [15] [18] a subband ED based sensing method, Max-Min ED, was proposed and demonstrated to provide similar sensing performance as the best eigenvalue based methods, but with greatly reduced computational complexity. In Chapter 5 of this thesis, the Max-Min ED concept is extended for cooperative spectrum sensing scenarios [26]-[28].

2.2.3 Other Sensing Methods

Besides ED and covariance based approaches, there exist a wide variety of spectrum sensing methods. As depicted in the Figure 2.2, waveform based sensing, cyclo stationary based sensing, matched filter based sensing and higher-order statistics based sensing are few of them to be named. In waveform based sensing, correlation between the received signal and a known copy of a PU waveform specific pattern is used for identifying the possible presence of PU signal. Cyclostationary based sensing exploits the cyclostationary features of the PU signal. Matched filter based sensing is, in principle, the best available non-blind sensing techniques when the receiver knows the transmitted signal. Matched filter based sensing can ensure short detection time but it cannot be implemented in practice because sufficient information about the PU signal is not available in commonly considered CR scenarios [15].

2.2.4 Cooperative Spectrum Sensing

The practical wireless channel behavior restricts critically the sensing performance and makes reliable operation of spectrum sensing based CR a very challenging in many practical scenarios. In practical wireless channel there exists the multipath and shadowing and as result, the PU signal cannot always be seen by the SU sensing process. This is the so-called hidden node problem, which causes the sensing results to be unrealistic. To counteract the practical wireless channel behavior and to enhance detection performance, collaborative sensing approaches have been suggested in literature [4] [11]. Here, simple solution to counteract the practical wireless channel effects is the CSS and it can be implemented by simply exploiting cooperation among SUs. Particularly, cooperative strategies can be adopted to counteract channel effects by exploiting the SUs spatial diversity. In other words, CSS mitigates channel effects such as multipath fading and shadowing.

Our studies will mainly explore collaborative approaches i.e., CSS utilizing subband ED techniques [15] [16] which have earlier been considered for single-station spectrum sensing only. Details on CSS will be covered in Chapter 3.

2.3 System Model

In this section, the system model used in later Chapters will be briefly explained. This includes the PU signal models and channel models.

2.3.1 PU Signal Models

Various PU signal models have been considered in these studies. The traditional approach of spectrum sensing is tested with three different signal models, quadrature phase shift keying (QPSK), 16-quadrature amplitude modulation (QAM) and 64-QAM. Additionally,

OFDM and FBMC waveforms are included in the evaluation of subband based spectrum sensing techniques as realistic signal models. Details of multicarrier based PU signal models will be covered in Section 4.1.2

2.3.2 Channel Model and Pathloss

Various channel models will be applied in these studies, including different multipath delay profiles, path loss models, and noise effects. Traditional spectrum sensing considered in these studies is modeled with two channel configuration. Model 1 includes log-normal path loss with AWGN whereas model 2 includes frequency selective multipath channel, log-normal path loss and AWGN. Different channel models for the frequency selectivity includes Indoor, International Telecommunication Union (ITU)-R vehicular A and Stanford University interim (SUI)-I channel model [30]. Effects of the different channel scenarios are studied and analyzed in the following chapter.

The log-normal path loss can be modeled as follows:

Receiver signal strength can be written as:

$$PL = PL_f * \left(\frac{d_j}{d_0}\right)^a * \varphi \quad (2.9)$$

In dB scale this gives,

$$PL_{dB} = PL_{f,dB} + 10 * a * \log(d_j/d_0) + \varphi_{dB} \quad (2.10)$$

where, PL_f is path-loss at the reference distance d_0 , a represents path-loss exponent, d_j represents the distance of j^{th} CR receiver where each station separated by d_{step} , and φ represents the Gaussian random value with zero mean and standard deviation σ .

3. TRADITIONAL COOPERATIVE SPECTRUM SENSING

This chapter gives a layout of traditional CSS schemes which is a collaborative approach among SUs to counteract practical wireless channel effects. Cooperation between CR receivers to enhance the detection performance is the main objective of these studies.

This chapter introduces:

- General information on traditional CSS schemes,
- Different linear fusion rules and their characteristics,
- Comparison of linear fusion rule on different channel models, and
- Optimized fusion rules that enhances the performance.

The chapter consists of six sections. Section 3.1 introduces and gives the general description of the traditional ED based CSS approach. Section 3.4 gives the layout of CSS algorithms and presents the block diagram representation of CSS approach. Section 3.2 gives the general idea about cooperative strategies implemented at the fusion center (FC). Section 3.3 gives the general idea about hard decision fusion and linear fusion rules implemented at the FC. Section 3.5 presents the results and analysis. Finally, summary is given in the last section.

3.1 Introduction

As already described earlier, CR technology provides a potential solution to the spectrum scarcity by enabling opportunistic usage of the spectrum. Radio scene analysis is one of the important functions of CR technology, which is however facing challenges with practical wireless channel's behavior. Practical wireless channel shows characteristics like noise uncertainty, multipath fading, and shadowing. In order to mitigate the effects of practical wireless channel, cooperation among many CR users i.e., CSS is considered. CSS is regarded as the potential solution to mitigate effects of both multipath and shadowing which causes the hidden node problem. It also enhances the detection performance and reliability [4]-[9].

As suggested in literature [11][12], the cooperative scheme can help to mitigate effects of the hidden node problem. Spatial diversity among all receiver is achieved, as illustrated

in Figure 3.1. The concept of exploiting SUs spatial diversity to counteract the hidden node effects and enabling cooperation among SUs is coined as CSS and has reached growing attention in recent years. Our studies consider the ED based CSS approach with hard decision combining. Hard decision combining refers to the combination of binary decisions from spatially separated CR receivers at the FC [14] [21].

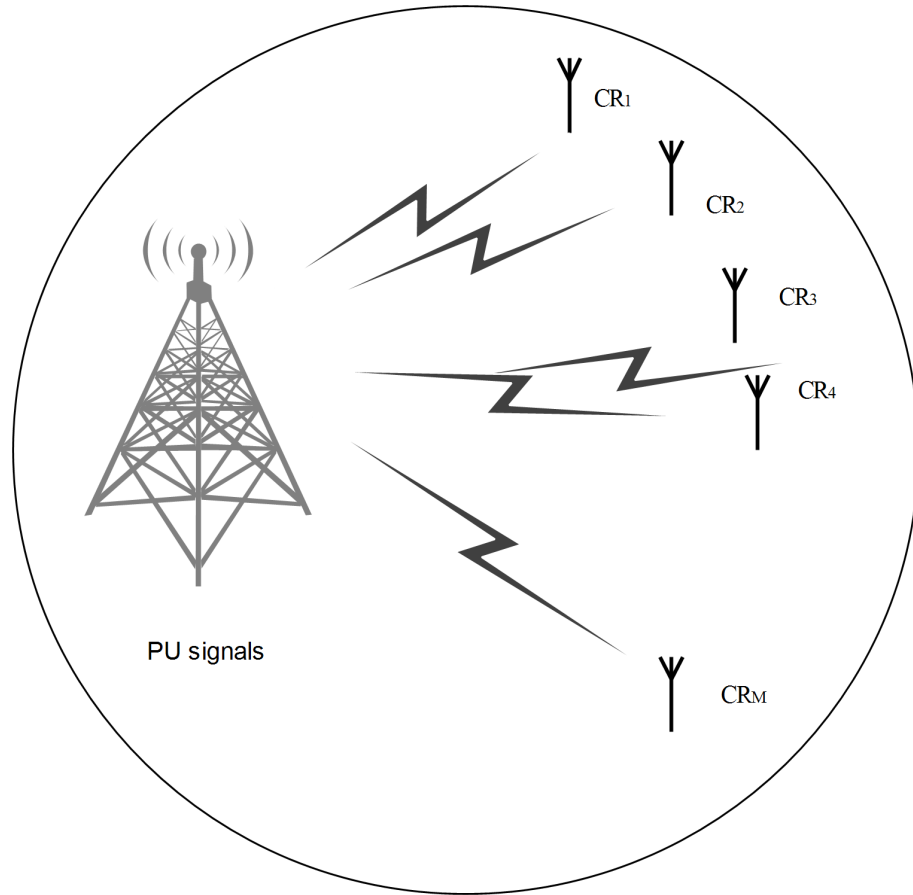


Figure 3.1: CR topology including PU signals and M CR users

CSS uses two or more CRs to combine their sensing result so as to increase the reliability of the result. Combining of result from different CR receivers is performed at FC. Different rules may be applied to combine the individual sensing results so as to achieve highest accuracy at FC. With an increase in a number of CR users, CSS could go through a complex procedure. Additionally, implementation cost increases with higher number of CR receivers. On the other hand, sufficient number of sensing CR stations is needed to reach sufficient sensing performance. So there is a trade-off between sensing performance and complexity of the CSS system. With increased number of CR receiver sensing performance enhances significantly. Performance parameters like sensing time and reliability are improved.

3.2 Cooperative Strategies

Cooperative networks can be classified on the basis of their data sharing methods among SUs and the point of final decision. Cooperative strategies can be classified as centralized cooperative sensing, distributed cooperative sensing, and mixed strategy. Centralized cooperative sensing collects the SUs data and makes the collaborative decision at FC. This approach of taking a collective decision at FC is called as centralized cooperative sensing. In case of distributive cooperative strategy, SUs independently take their own decisions and forward them to the FC. FC then combines the forwarded decision to make a collective decision. SUs can also coordinate the neighbor SUs to make their own decision on presence of PU. Both strategies can also be mixed for better cooperation between SUs. For SUs having weak signal strength at the FC, relay assisted cooperative scheme can be implemented to compensate the weak channel effects and the rest of the SUs can send their information directly to the FC. This type of mixed approach is called mixed strategy in CSS. Additionally, cooperative schemes can also be classified as hard and soft fusion schemes. When CRs provide binary information about the presence of PUs, FC applies hard fusion rules CRs may provide reliability information about their sensing results in the form of non-binary soft decisions, in which case FC applies soft fusion scheme [4].

3.3 Hard Decision Fusion with Linear Fusion Rules

Hard fusion can be implemented using linear rules such as "AND rule", "OR rule", "Majority rule". Hard decision fusion does not need to exchange the data among secondary nodes. Soft schemes generally improve the sensing result by sending richer information to the FC. Soft fusion techniques increase the complexity compared to hard fusion techniques [21].

Linear fusion rules are applied by the FC to exploit the cooperation among CR receivers. Binary decision from independent CR receivers is forwarded to the FC. FC processes the decisions from all CRs to make the collective decision. Linear fusion rules are based on the general " k -out-of- M rule". When k is equal to one i.e., 1 -out-of- N , the rule is equivalent to "OR rule". When k is equal to M i.e., M -out-of- M , the rule is equivalent to "AND rule". Whereas $M/2$ -out-of- M is special case and is known as "Majority rule". In "Majority rule" k equals to the half of the CRs. Different linear rules have unique attributes, for example "OR rule" has high detection probabilities and high false alarm, whereas "AND rule" has the lowest detection and false alarm probabilities. However "Majority rule" has moderate performance compared to both "OR rule" and "AND rule" FC [21][22].

Additionally, the three different rules have been studied in this work and the result will be presented in Section 3.5.

3.3.1 OR Rule

"OR rule" is one of the fusion rules which is applied at FC. When at least one SU detects the PU signal, "OR rule" declares the presence of PU. With M number of SUs, the cooperative detection probability $P_{D,t}$ and false alarm probability $P_{FA,t}$ at the FC are computed as follows,

$$\text{OR-Rule : } \begin{cases} P_{D,t} = 1 - (1 - P_D)^M \\ P_{FA,t} = 1 - (1 - P_{FA})^M \end{cases} \quad (3.1)$$

where, $P_{D,t}$ and $P_{FA,t}$ are collaborative detection and false alarm probabilities achieved after implementation of "OR rule" at FC. P_D and P_{FA} are the detection and false alarm probabilities of individual SUs reported to the FC.

"OR rule" has very high detection probability which is helpful to protect the primary user. Additionally, the false alarm is relatively high which makes the opportunistic spectrum usage inefficient [13].

3.3.2 AND Rule

"AND rule" declares the presence of PU signal if and only if all SUs detect the PU signal individually. With M SUs at FC, the detection probability $P_{D,t}$ and false alarm probability $P_{FA,t}$ at a FC are computed as follows,

$$\text{AND Rule : } \begin{cases} P_{D,t} = P_D^M, \\ P_{FA,t} = (P_{FA})^M. \end{cases} \quad (3.2)$$

This results suggests that "AND rule" has very low false alarm which makes spectrum usage efficient, on contrary it also has low detection probability hence it may not protect the PU from strong interference from the SUs. As a result, the quality of services for PU can not be guaranteed [13].

3.3.3 Majority-Rule

According to the studies, both "AND rule" and "OR rule" equally limited in terms of detection and false alarm probabilities. Considering the limitation of both rule, from the generalized $k-out-of-M$ rule, half number of SUs are selected to decides the presence of PU signals. The rule is named as "Majority rule" as most of the SUs involve on decision making at FC. "Majority rule" shows moderate results compared to both "OR rule" and "AND rule". It can be regarded as a trade-off between the low detection probability of "AND rule" and high false alarm probability of "OR rule". Considering the M sensing stations in the CSS, the detection and false alarm probabilities of the "Majority rule" can

be written as follows:

$$M/2 - out - of - M Rule : \begin{cases} P_{D,t} = \sum_{j=M/2}^M \binom{M}{j} P_D^j (1 - P_D)^{M-j} \\ P_{FA,t} = \sum_{j=M/2}^M \binom{M}{j} (1 - P_{FA})^{M-j} P_{FA}^j \end{cases} \quad (3.3)$$

here number of sensing stations are equal to M and is assumed even.

"Majority rule" is a special case of " $k - out - of - M$ rule" when $k = M/2$. If at least half of the SUs report the presence of PU, FC declares the presence of PU otherwise it declares that the spectrum is free to use for CR transmission [13] [14].

3.3.4 Generalized Rule of k-out-of-M

The generalized form of the linear rule can be defined by requiring k SUs to decide the presence of PU signal out of M SUs. Here number k can be any value between 1 to M , based on the requirements. As discussed earlier, the special cases $k = 1$, $k = M/2$, and $k = M$ are equivalent to "OR rule", "Majority rule" and "AND rule", respectively. Nevertheless, the number k can be optimized according to the targeted detection and false alarm performances [14][22].

$$K - out - of - M Rule : \begin{cases} P_{D,t} = \sum_{j=K}^M \binom{M}{j} P_D^j (1 - P_D)^{M-j} \\ P_{FA,t} = \sum_{j=K}^M \binom{M}{j} (1 - P_{FA})^{M-j} P_{FA}^j \end{cases} \quad (3.4)$$

3.3.5 Optimized k-out-of-M Rule

The " $k - out - of - M$ rule" estimates the presence of PU when k or more SUs report the presence of PU. Values of k can be set according to the system requirements. Optimized k for specified P_D and P_{FA} can be evaluated from equation as follows:

$$K_{opt} = \frac{\ln \left(\frac{P(\mathcal{H}_1) (1 - P_D)^M}{P(\mathcal{H}_0) (1 - P_{FA})^M} \right)}{\ln \left(\frac{P_{FA} (1 - P_D)}{(1 - P_{FA}) P_D} \right)}. \quad (3.5)$$

where $P(H_1)$ and $P(H_0)$ represents present and absent hypothesis probability. Table 3.1 shows the optimized value of k for different parameters [14][22].

Table 3.1: Optimized K for different M , P_D and targeted P_{FA} . Here hypothesis probability is assumed as $P(H_1) = P(H_0) = 0.5$.

M	$P_D=0.8$ $P_{FA}=0.2$	$P_D=0.9$ $P_{FA}=0.1$	$P_D=0.95$ $P_{FA}=0.05$	$P_D=0.9$ $P_{FA}=0.01$
8	4	4	5	2
15	8	10	11	5
19	10	13	14	6
23	12	15	17	7
35	13	16	18	8

3.4 Traditional CSS Algorithms

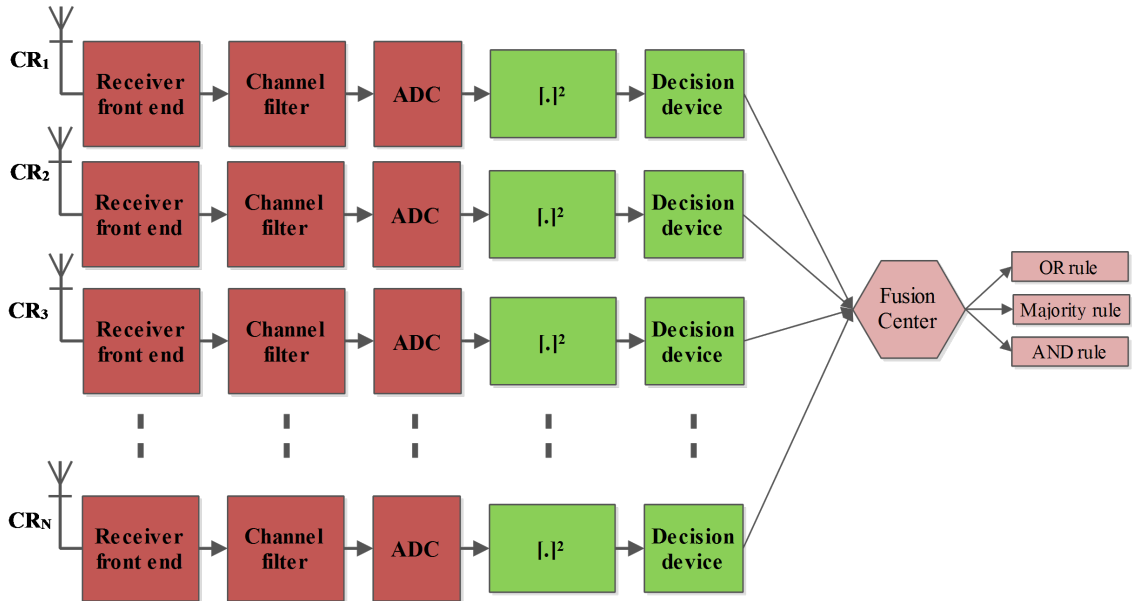


Figure 3.2: Block diagram of traditional cooperative spectrum sensing techniques

Traditional CSS starts with the receiver front end as depicted in Figure 3.2. SU after receiving PU signal does the channel filtering. The digital conversion of the analog signal is done through analog-to-digital converter (ADC). The test statistics are obtained by taking the average of the squared magnitude values over the observation interval of N samples. The decision device of each SU estimates the presence of the PU. Here the signal energy is compared against a predefined threshold. When the energy statistic is higher than the threshold, the presence of the PU is decided, otherwise it is assumed to be

absent. Decisions from all individual CR receivers are forwarded to the FC. FC applies linear fusion rules to combine the decisions from individual CR receivers. As seen in Figure 3.2, three different linear fusion rules have been implemented at the FC.

CSS exploits the spatial diversity among CR receivers. CSS can counteract the practical wireless channel effects, both the hidden node problem and the multipath effects. Additionally, the reliability of spectrum sensing is also increased with the increasing of number of CR receivers. Traditional CSS algorithms have been analyzed with the help of receiver operating characteristics (ROC) curves under different false alarm probabilities. A ROC curve gives the detection probability as a function of the false alarm probability. Plots of detection probability over different SNR levels have also been considered in these studies.

3.5 Simulation Results

The section presents simulation results for traditional CSS techniques with linear fusion rules. Simulations carried out for two different scenarios, both including log-normal shadow-fading but with or without frequency selective channel model. The following section presents the detail analysis.

3.5.1 Log-Normal Pathloss with AWGN

The performance of traditional ED based CSS for frequency-flat lognormal fading is presented in this section. In test scenario, the number of sensing stations equal to $M = 8$, the sample complexity $N = 10240$. For flat-fading log-normal path loss model, only Gaussian random variable is considered. P_{FA} for each sensing station is equals to 0.01. For the PU signal simplified model of QPSK, 16-QAM and 64-QAM constellations is considered. For non-oversampling PU signal model no filtering and modulation are used. For 2x-oversampling PU model, root-raised cosine filtering is considered with 22 % of roll-off factor.

Figure 3.3 shows the detection probabilities with three different fusion rules for different PU signal models: QPSK, 16-QAM and 64-QAM. The figure shows, 90 % detection probability for "OR rule" is achieved at $\gamma = -21$ whereas for "Majority rule" and "AND rule" 90 % detection probability are achieved at $\gamma = -15$ and -3 dB, respectively. Figures show, detection performance is same irrespective of PU signal model cases.

ROC curve for 16-QAM PU signal model at $\gamma = -15$ dB with three different linear fusion rules are presented in Figure 3.4. AWGN noise without frequency selective channel with frequency-flat log-normal fading with 6 dB standard deviation is considered. ROC curve gives the trade off between detection probability P_D and false alarm probability P_{FA} . The figure shows, "OR rule" has detection probability very close to 1 even with very small false alarm probabilities, much less than 0.1 and outperform both Majority and

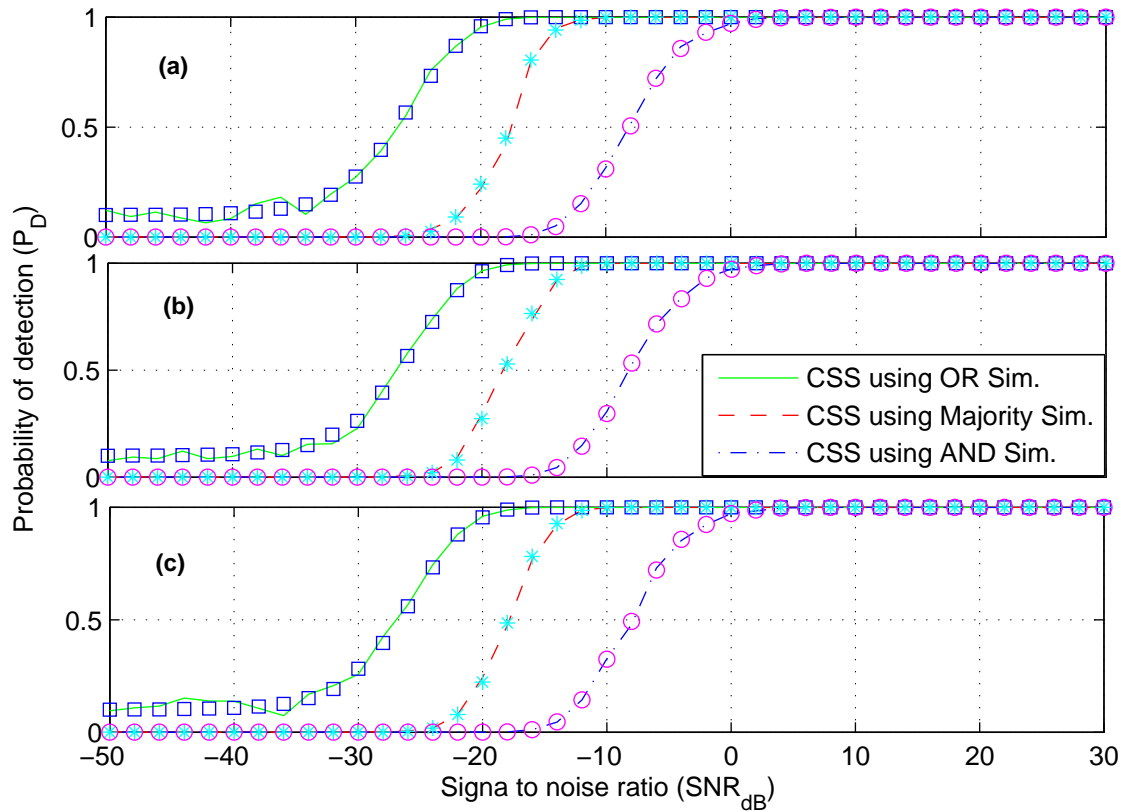


Figure 3.3: CSS detection probabilities against SNR with basic ED and three different linear fusion rules for a channel with frequency-flat log-normal fading with 6 dB standard deviation. The sample complexity is $N = 10240$, the number of sensing stations $M = 8$, $P_{FA} = 0.01$ for each station. a) QPSK, b) 16-QAM and c) 64-QAM.

AND rules. "Majority rule" shows better detection probabilities compared to "AND rule" and 90 % P_D is achieved at $P_{FA} = 0.01$.

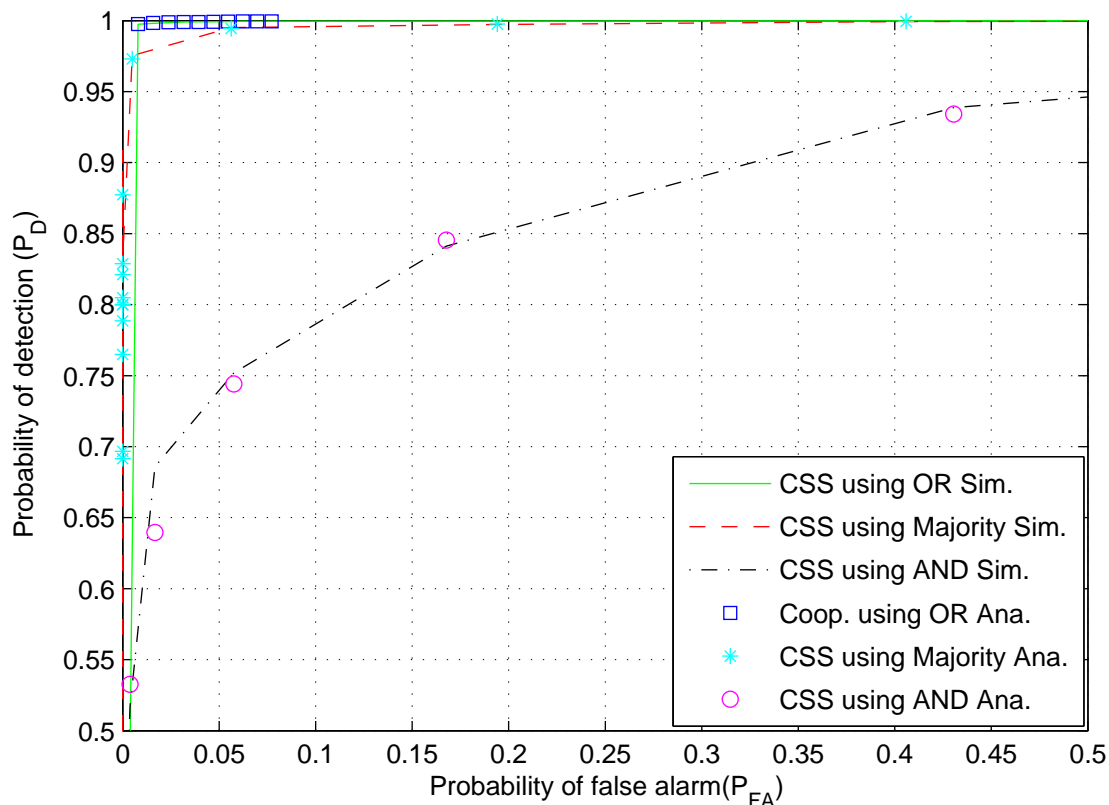


Figure 3.4: ROC curve at $\gamma = -15$ dB with basic ED and three different linear fusion rules for a channel with frequency-flat log-normal fading with 6 dB standard deviation. PU signal model is 16-QAM, the sample complexity is $N = 10240$, the number of sensing stations $M = 8$.

Detection probabilities with three different fusion rules for 16-QAM PU signal model for frequency-flat log-normal fading with standard deviation of 9 dB is presented in Figure 3.5. 90 % detection probability is achieved at SNR equals to -23 dB, -14 dB and 7 dB respectively for "OR rule", "Majority rule" and "AND rule".

ROC curve for 16-QAM PU signal model at $\gamma = -13$ dB for frequency-flat log-normal fading with standard deviation of 9 dB is presented in Figure 3.6. It shows that "OR rule" has detection probability very close to 1 even with very small false alarm probabilities, much less than 0.01. On other hand, "AND rule" has very low detection probability even with higher false alarm probabilities.

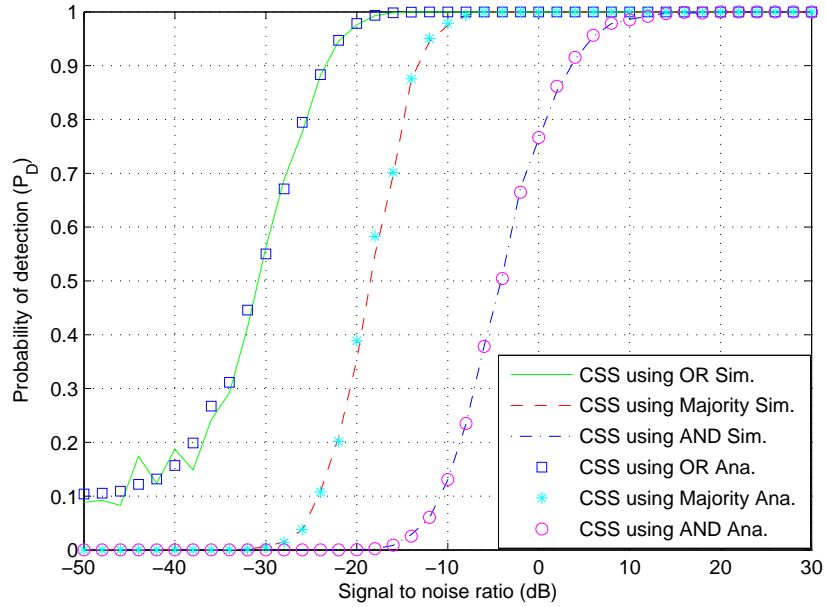


Figure 3.5: CSS detection probabilities against SNR with basic ED and three different linear fusion rules for a channel with frequency-flat log-normal fading with 9 dB standard deviation. PU signal model is 16-QAM, the sample complexity is $N=10240$, the number of sensing stations $M=8$, and $P_{FA} = 0.01$ for each station.

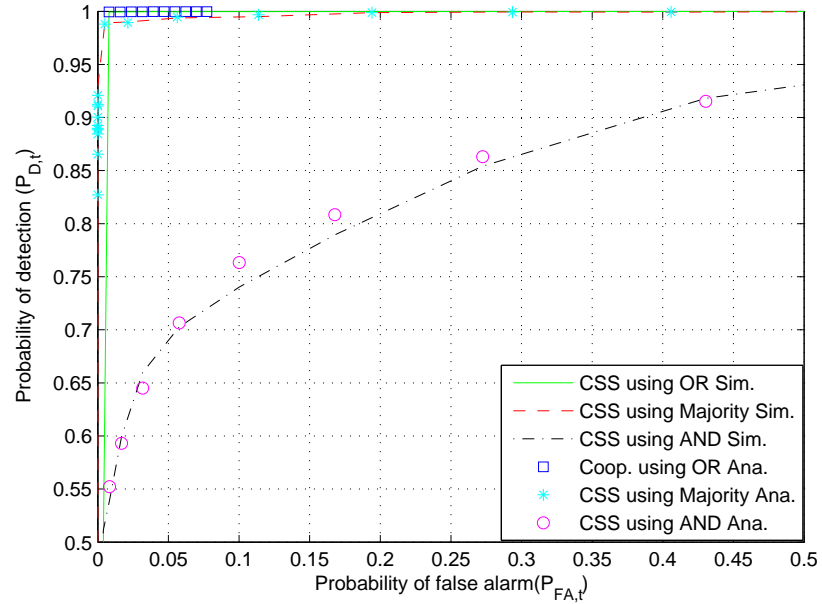


Figure 3.6: ROC curve at $\gamma = -13$ dB with basic ED and three different linear fusion rules for a channel with frequency-flat log-normal fading with 9 dB standard deviation. PU signal model is 16-QAM, the sample complexity is $N = 10240$, and the number of sensing stations $M = 8$.

3.5.2 Frequency Selective Channel

Traditional CSS techniques have been simulated for highly frequency-selective channels and log-normal path loss condition including AWGN. A practical wireless channel includes multipath propagation, which introduces frequency selectivity. In our second test scenario, Indoor, ITU-R Vehicular A, and SUI-1 [15] channel models are considered. PU signal is modeled as single-carrier transmission with 64-QAM modulation with the sample complexity $N = 10240$. In test scenario, 0 dB or no noise uncertainty is considered. The number of sensing stations equal to $M = 8$. Three different linear fusion rules are applied to exploit cooperation among different sensing station. Detection probabilities and ROC curves have been observed for the three different channel models.

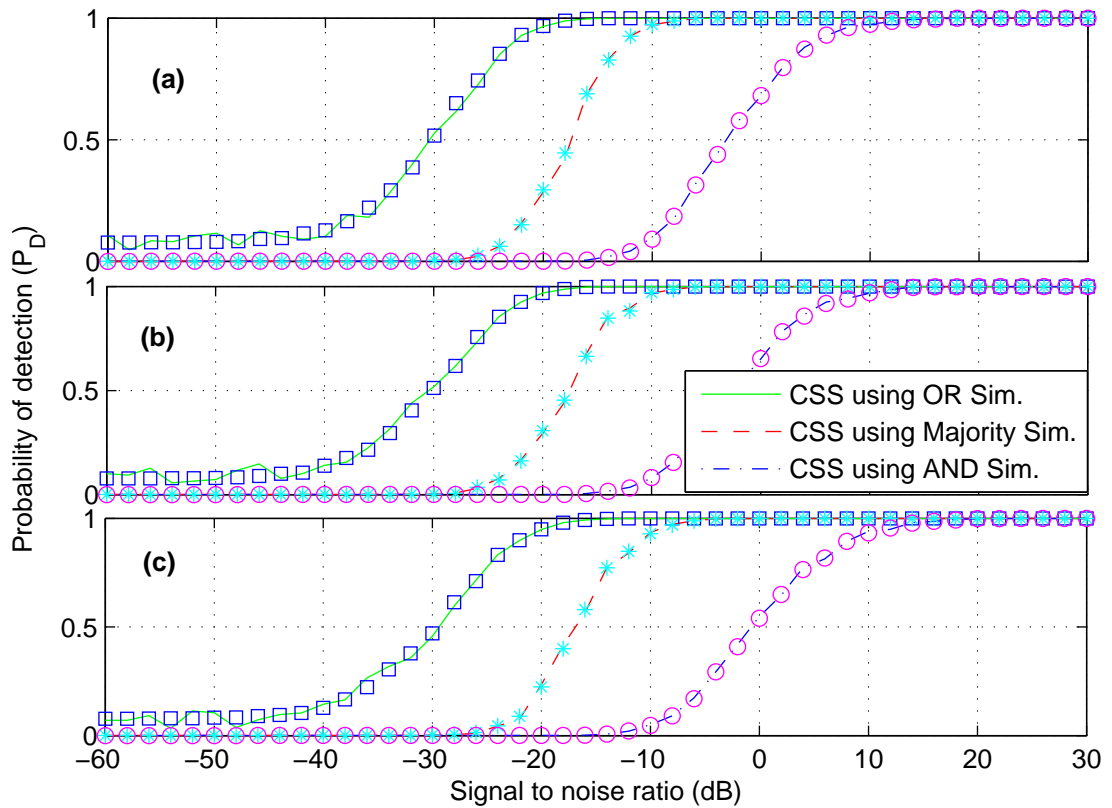


Figure 3.7: CSS detection probabilities with basic ED and three different linear fusion rules for frequency-flat log-normal fading with standard deviation 9 dB. PU signal model is 64-QAM, the sample complexity $N = 10240$, the number of sensing stations $M = 8$, and $P_{FA} = 0.01$ for each sensing station. a) Indoor channel, b) ITU-R vehicular A channel, and c) SUI-I channel.

Figure 3.7 shows the CSS detection probabilities with three different fusion rules for frequency-flat log-normal fading with 9 dB standard deviation for different frequency selective channels: a) Indoor channel, b) ITU-R vehicular A channel, and c) SUI-I channel.

Table 3.2: SNR values for 90 and 99% detection probability with three different fusion rules for frequency selective channels: a) Indoor, b) ITU-R vehicular A, and c) SUI-I channel.

	Fusion rule	Indoor channel	ITU-R vehicular A channel	SUI channel
$P_D = 0.9$	"OR rule"	-23 dB	-23.5 dB	-21 dB
	"Majority rule"	-12.5 dB	-11.5	-11 dB
	"AND rule"	5 dB	6 dB	8 dB
$P_D = 0.99$	"OR rule"	-18 dB	-17 dB	-16 dB
	"Majority rule"	-7 dB	-7 dB	-5 dB
	"AND rule"	13 dB	13 dB	17 dB

With frequency selective channel, the detection performance of the traditional ED based spectrum sensing is improved. Indoor channel with high selectivity, shows better detection performances compared to both ITU-R vehicular A and SUI-I channel. 90 and 99% detection probabilities for three different channels with three fusion rules are presented in Table 3.2.

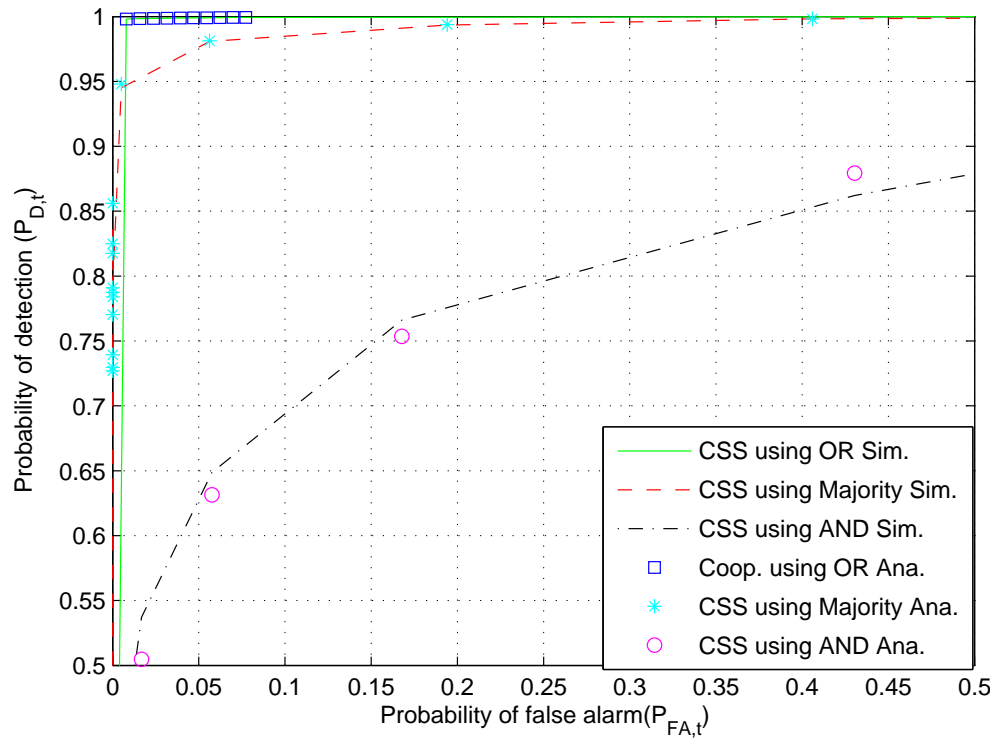


Figure 3.8: ROC curve at $\gamma = -14$ dB with basic ED and three different linear fusion rules for the Indoor channel with frequency-flat log-normal fading with standard deviation 9 dB. PU signal model is 64-QAM, the sample complexity $N = 10240$, and the number of sensing stations $M = 8$.

CSS ROC curves with basic ED with three different linear fusion rules for Indoor,

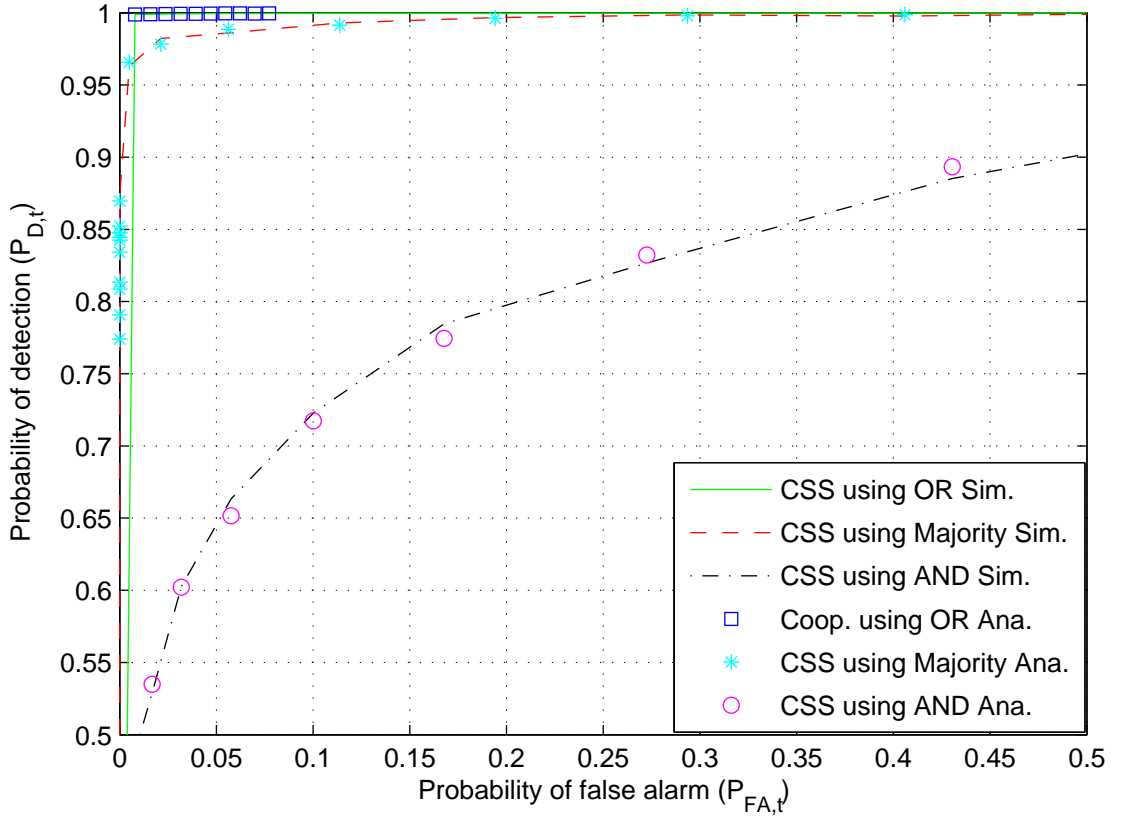


Figure 3.9: ROC curve at $\gamma = -13$ dB with basic ED and four different linear fusion rules for the ITU-R vehicular A channel with frequency-flat log-normal fading with standard deviation 9 dB. PU signal model is 64-QAM, the sample complexity $N = 10240$, and the number of sensing stations $M = 8$.

ITU-R vehicular A and SUI-I channels with frequency-flat lognormal fading with standard deviation 9 dB are shown in Figure 3.8, 3.9 and 3.10, respectively. These Figures reflect fundamental tradeoff between P_D and P_{FA} . Figures show, "OR rule" has detection probability very close to 1 even with very small false alarm probabilities, much less than 0.1. On other hand, "AND rule" has the lowest detection probabilities even with high false alarm probabilities.

Hard decision combining for three different linear fusion rules are presented in this thesis. Results presented in this thesis might not give the fair comparisons for the cooperative sensing algorithms. However, the fair comparison can be done with fusion center P_{FA} for each linear fusion rule. In the fair comparison, results may vary as presented in this thesis.

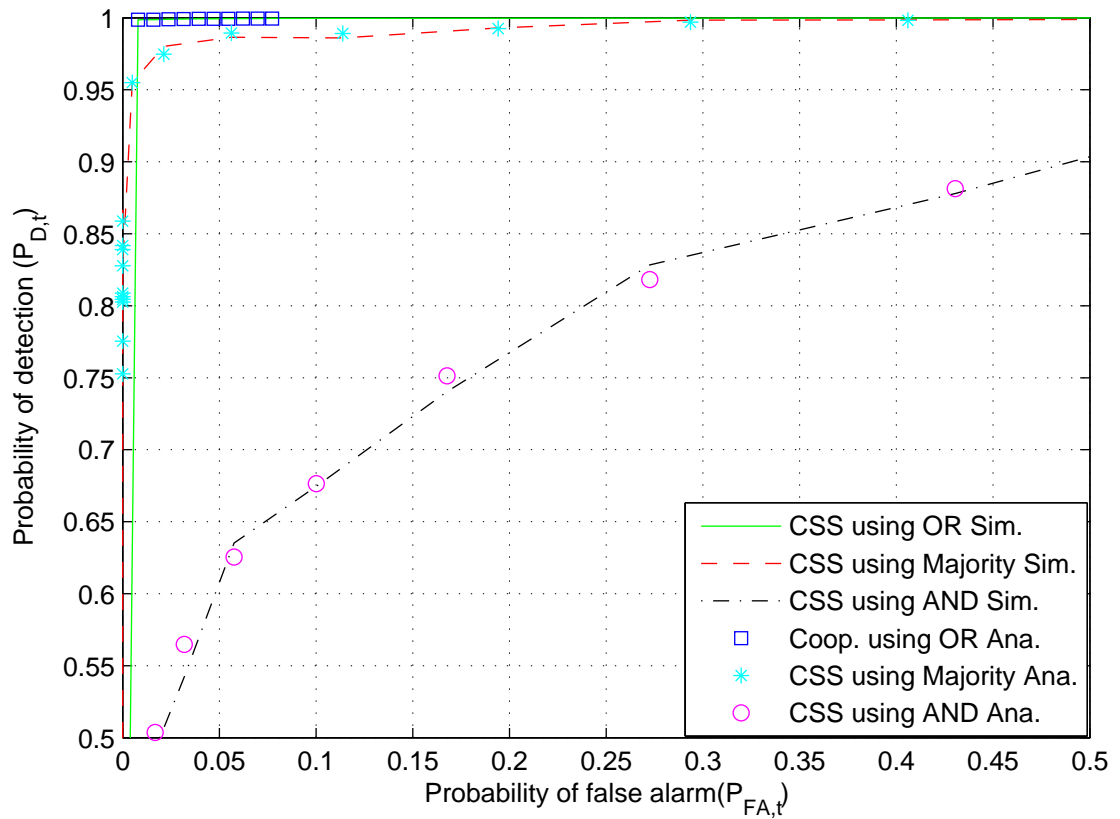


Figure 3.10: ROC curve at $\gamma = -12$ dB with basic ED and three different linear fusion rules for the SUI-1 channel with frequency-flat log-normal fading with standard deviation 9 dB. PU signal model is 64-QAM, the sample complexity $N = 10240$, and the number of sensing stations $M = 8$.

3.6 Chapter Summary

In this chapter ED based traditional CSS methods were presented. The idea behind the traditional CSS was to exploit the collaboration among the number of spatially separated CR receivers. CSS helped to eliminate the both hidden node and multipath problems. The frequency-flat log-normal fading effect was considered for different frequency selective channel models: Indoor, ITU-R vehicular A and SUI-I channels. Cooperation among the number of sensing stations were done with different linear fusion rules such as: "OR rule", "AND rule", and Majority rule. Performances of traditional CSS algorithm with different linear fusion rule on frequency selective channel was presented in this chapter. With high selectivity, Indoor channel has the better performance compared to other frequency selective channels. With the increasing number of CR the detection performance can be enhanced. Linear fusion rule for different channel and fading condition were presented.

4. PROPOSED FFT AND AFB BASED COOPERATIVE SPECTRUM SENSING

In this chapter, efficient subband based ED methods are proposed for spectrum sensing. The aim of the study is to investigate the effects of practical wireless channels on the ED performance and quantify the corresponding deviations from the ideal model. Specifically, the following topics will be covered:

- Basics of FFT/AFB and multicarrier systems,
- Effects of practical wireless channels on the subband based ED,
- Application of subband based sensing in CSS is proposed.

The chapter consists of four different sections. Section 4.1 covers the basics of FFT and AFB, including also short introduction of the related multicarrier transmission systems. Section 4.2 covers the FFT/AFB based sensing algorithms. Section 4.3 proposes the FFT/AFB based CSS algorithm. Section 4.4 presents the result and analysis of the proposed algorithm. At last, conclusion are presented in the section 4.5.

4.1 Introduction

Efficient spectrum sensing is the most important step in CR to maintain its proper operation. To address issues like channel effects in traditional spectrum sensing, efficient subband based technique has been emerged in the field of CR technology. In recent years, the OFDM multicarrier modulation technique has been widely adopted for broadband wireless services. However, alternative technique, FBMC waveform shows greater performance in terms of spectral efficiency compared to that of cyclic prefix based orthogonal frequency division multiplexing (CP-OFDM). FBMC is one of the promising multicarrier techniques in CR based technology. Consequently, FBMC is regarded as an alternative multicarrier techniques for next-generation wireless communications, 5G. The concept of FBMC includes synthesis filter bank (SFB) as core elements on the transmitter and AFB on the receiver side. In CR based transmission, the FFT processing in OFDM or the AFB processing in FBMC on the receiver side can be used for spectrum sensing purposes. AFB has significant benefits in spectrum sensing due to the much better spectral containment of the subbands.

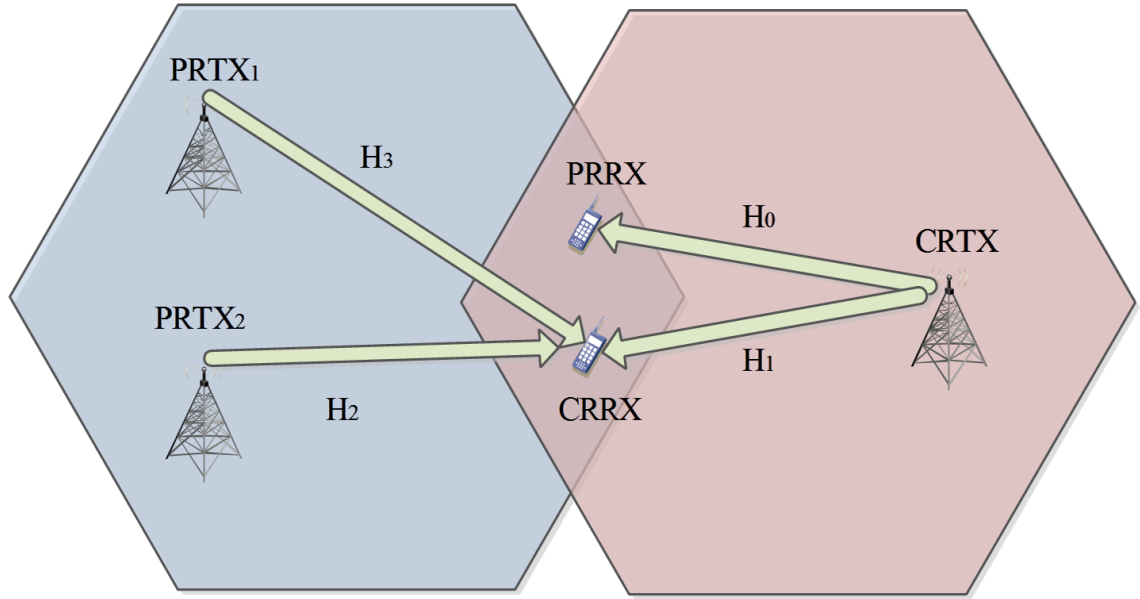


Figure 4.1: System model for spectrum sharing in CR.

The non-cooperative CR system model is depicted in Figure 4.1, where the PU and CR systems are working in the same band of frequencies. In this figure PU and CR transmitters are represented as PRTX and CRTX, respectively. The receivers are represented as PRRX and CRRX, accordingly. Frequency-selective channels between the PU and CR stations are denoted as H_0 , H_1 , H_2 and H_3 . As seen in the figure, the CR system is operating in a spectrum gap next to relatively strong on-going primary communications on either or both sides of the gap. This led us to the conclusion that interference is unavoidable between different PUs and CRs. Spectrum sensing hence has the main function of detection of possible other transmissions or reappearing PUs within the spectrum gap. Furthermore, the stations of the CR system are assumed to have means to exchange control information with each other, e.g., using a cognitive control channel [15].

Additionally, interference model between PUs is covered in this section. Figure 4.2 indicates the gap in between two PU signal models and the exploiting SUs in between the gap. B represents the available bandwidth for the secondary communication under the number of holes between two PU signals. However, there exist the interference leakage effects and the interference can be modeled as $I_k(P_k) = P_k \Omega_k$. Here P_k is sub-carrier power and Ω_k is combined interference factor for k^{th} sub-carrier [15].

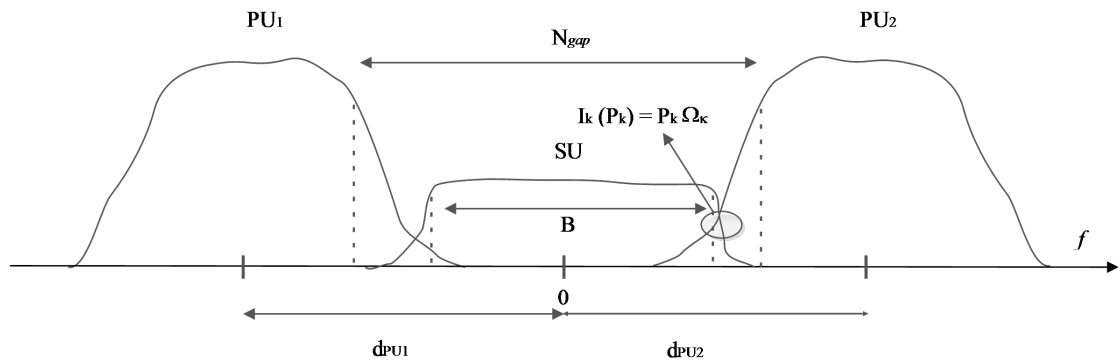


Figure 4.2: Interference model between primary and secondary users

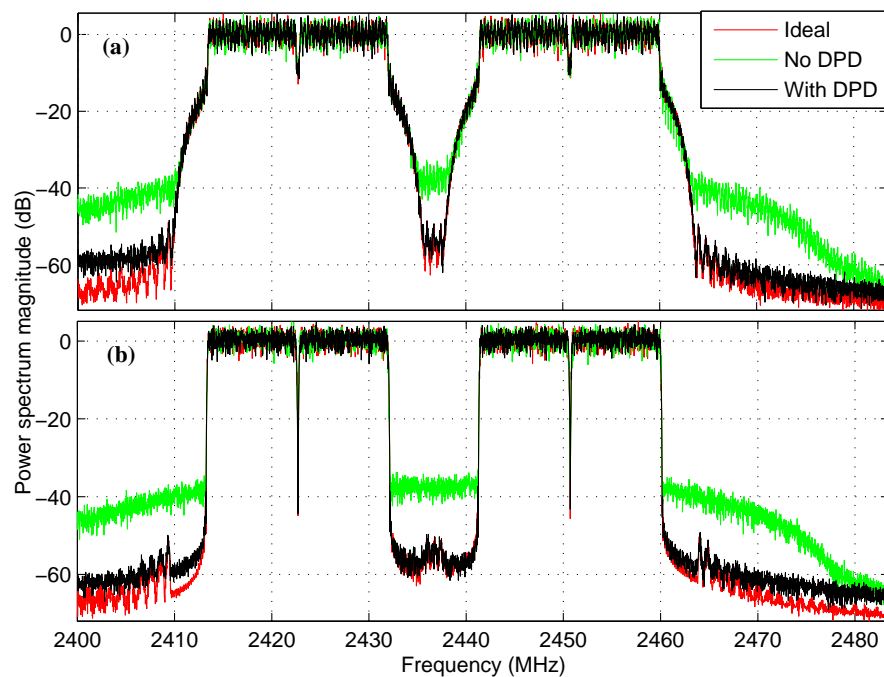


Figure 4.3: Effects of the power amplifier model on (a) OFDM and (b) FBMC based PUs spectra.

4.1.1 FFT and AFB Basics

Fourier transform is a mathematical transformation and is widely used for transforming signals between time and frequency domain and vice-versa in communication signal processing. The discrete Fourier transform (DFT) is used for the finite sequences of equally spaced samples and FFT is an efficient algorithm to compute the DFT and its inverse. In spectrum sensing, FFT is used to split a wideband signal into a number of equally spaced subbands and to use them for further processes within the sensing algorithm. In communication signal processing, an array of band-pass filters is commonly known as

filter bank. In the spectrum sensing context, AFB is used to separate the input signal samples into subbands each carrying different frequency components. SFB can be used for constructing a time-domain signal from the subbands [16] [33].

4.1.2 Multicarrier Systems

OFDM with cyclic prefix i.e., CP-OFDM is the dominating multicarrier technology in the field of wireless communication. Additionally, discrete wavelet multitone (DWMT), cosine modulated multitone (CMT), filtered multitone (FMT), and OFDM with offset QAM are commonly used alternative forms of multicarrier techniques [23] [24]. OFDM based multicarrier is primarily considered in the study of this thesis. Recently FBMC based model is emerging as a promising multicarrier model that is applicable to CR based technology. FBMC shows the better spectral efficiency compare to the CP-OFDM. Unlike the CP-OFDM, FBMC avoids the cyclic prefix overhead. Additionally, the frequency overhead due to guard-bands is reduced. However, FBMC based model is computationally more complex comparing with CP-OFDM models [25].

Both inverse fast Fourier transform (IFFT) and SFB are considered as transmitter side elements whereas FFT and AFB are considered as receiver side elements. In this study, FFT processing of OFDM based multicarrier and AFB processing of FBMC based multicarrier is considered. Subband based ED can be used in wideband spectrum sensing which covers the multiple frequency bands or the whole service band in multicarrier based cases. AFB with better spectral containment is an efficient receiver side processing technique compared to FFT based receiver side processing technique. Here in this study, filter banks with 50 dB stop band attenuation are considered [15]. FBMC hence can be used efficiently in CR system with narrow spectral gaps [25] [24].

4.2 FFT and AFB based Energy Detector Algorithms

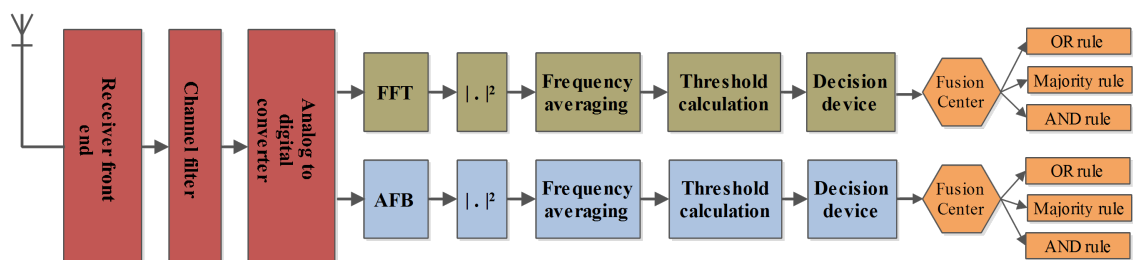


Figure 4.4: Block diagram of alternative filter bank (AFB) and fast Fourier transform (FFT) based spectrum analysis methods for subband energy based cooperative sensing schemes.

FFT and AFB techniques are applied to the wideband signal to generate equally spaced subband signal. Subband energies are calculated by the subband energy detector (SED). Subband energies are processed accordingly to apply the ED based sensing algorithms. The entire procedure is represented in Figure 4.4. The receiver front end collects the PU signals which is followed by channel filter. The channel filter output is fed to the ADC to convert into discrete sequence so as to generate equally spaced subbands as described earlier. subbands can be obtained either via FFT or AFB and then processed accordingly [17].

A subband signal can be represented as follows,

$$Y_k[m] = \begin{cases} \mathcal{W}_k[m] & \mathcal{H}_0, \\ S_k[m]H_k + \mathcal{W}_k[m] & \mathcal{H}_1. \end{cases} \quad (4.1)$$

Here $S_k[m]$ is the transmitted signal by PUs as it appears at the m^{th} FFT or AFB output sample in subband k and $\mathcal{W}_k[m]$ is the corresponding channel noise sample. \mathcal{H}_1 illustrates the *present hypothesis* of a PU signal whereas \mathcal{H}_0 illustrates the *absent hypothesis* of a PU signal. When the AWGN only is present, the white noise is modeled as a zero-mean Gaussian random variable with variance σ_w^2 i.e., $\mathcal{W}_k[m] = \mathcal{N}(0, \sigma_w^2)$. The OFDM and FBMC signals can also be modeled as a zero-mean Gaussian variables $S_k[m] = \mathcal{N}(0, \sigma_k^2)$ where, σ_k^2 is the variance (power) at subband K . The subband energy is calculated from the subband signal in Equation 4.1. Subband energy is sent to a threshold block to detect the possible occupancy of the corresponding frequency band at that time interval. Integrated test statistics can be calculated as follows,

$$T(y_{m_0}, k_0) = \frac{1}{N_t N_f} \sum_{k=k_0 - [N_f/2]}^{k_0 + [N_f/2] - 1} \sum_{m=m_0 + N_t + 1}^{m_0} |y_k[m]|^2. \quad (4.2)$$

here N_f and N_t are the averaging filter lengths in the frequency and time domain, respectively. Test statistic over subband is calculated by integrating over the time. Spectral components are entirely captured within the subband integration range. Assuming flat PU spectrum over the sensing band, the probability distribution of the test statistics can be expressed as,

$$\begin{aligned} T(y_{m_0}, k_0) | \mathcal{H}_0 &\sim \mathcal{N}\left(\sigma_{w,k}^2, \frac{\sigma_{w,k}^4}{N_t N_f}\right) \\ T(y_{m_0}, k_0) | \mathcal{H}_1 &\sim \mathcal{N}\left(\sigma_{x,k}^2 + \sigma_{w,k}^2, \frac{(\sigma_{x,k}^2 + \sigma_{w,k}^2)^2}{N_t N_f}\right) \end{aligned} \quad (4.3)$$

which yields,

$$\begin{aligned}
P_{FA} &= P_r(T(y) > \lambda | \mathcal{H}_0) = Q\left(\frac{\lambda - \sigma_{w,k}^2}{\sigma_{w,k}^2 / \sqrt{N_f N_t}}\right) \\
P_D &= P_r(T(y) > \lambda | \mathcal{H}_1) = Q\left(\frac{\lambda - \sigma_{w,k}^2(1 + \gamma_k)}{\sigma_{w,k}^2(1 + \gamma_k) / \sqrt{N_f N_t}}\right)
\end{aligned} \tag{4.4}$$

where λ is calculated as,

$$\lambda = \sigma_{w,k}^2 \left(1 + \frac{Q^{-1}(P_{FA})}{\sqrt{N_f N_t}}\right). \tag{4.5}$$

Here, $\gamma_k = \sigma_{x,k}^2 / \sigma_{w,k}^2$ is the SNR of subband k . With FFT/AFB based processing it is possible to tune the sensing frequency band to the expected band of the PU signal and sensing multiple PU bands simultaneously.

4.3 FFT/AFB based cooperative spectrum sensing

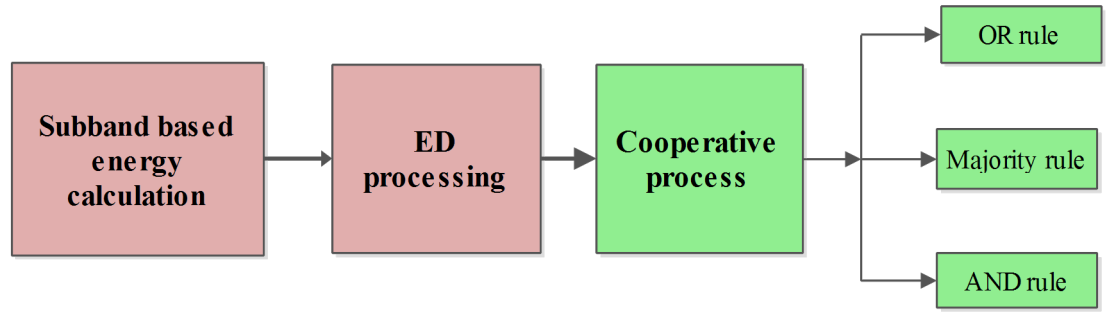


Figure 4.5: Block diagram of fast Fourier transform (FFT) and analysis filter bank (AFB) based cooperative spectrum technique.

Cooperation among number of sensing stations with FFT and AFB based spectrum sensing is covered in this section. Cooperative process is depicted in Figure 4.5. As described earlier in the study of this thesis, three linear fusion rules have been proposed for combining the binary decisions that are forwarded to the FC. Here, three different fusion rules, "OR rule", "Majority rule" and "AND rule", are considered for the false alarm probabilities. False alarm probabilities with three different linear fusion rules are calculated as follows,

$$P_{FA,t} : \begin{cases} = 1 - (1 - P_{FA})^M & \text{"OR rule"} \\ = P_{FA}^M & \text{"AND rule"} \\ = \sum_{j=M/2}^M \binom{M}{j} P_{FA}^j (1 - P_{FA})^{M-j} & \text{"Majority rule"} \end{cases} \tag{4.6}$$

Here $P_{FA,t}$ is cooperative false alarm probability and P_{FA} is non-cooperative false alarm probability.

4.4 Simulation Results

In this study, the potential spectral hole between two relatively strong PUs is determined by the spectrum sensing function of CR, as indicated in Figure 4.3. Additionally, it is assumed that there is no additional signal in the spectral hole. However, the spectrum sensing gives false alarm probabilities due to the spectral leakage of power amplifier non-linearity on PU. Such an effect is found to be dependent on the SNR values of the PUs. Furthermore, smaller subband spacing of 81.5 kHz for the spectrum sensing and the CR transmissions is assumed, instead of the 325 kHz sub-carrier spacing of wireless local area network (WLAN), in an attempt to reduce the effects of frequency selective channels. The time averaging lengths of 50 and frequency averaging length of 5 have been chosen in this scenario. The power amplifier non-linearity introduces interference leakage to the spectrum gap between the PUs, as illustrated in Figure 4.3, and the width of the spectral hole is reduced.

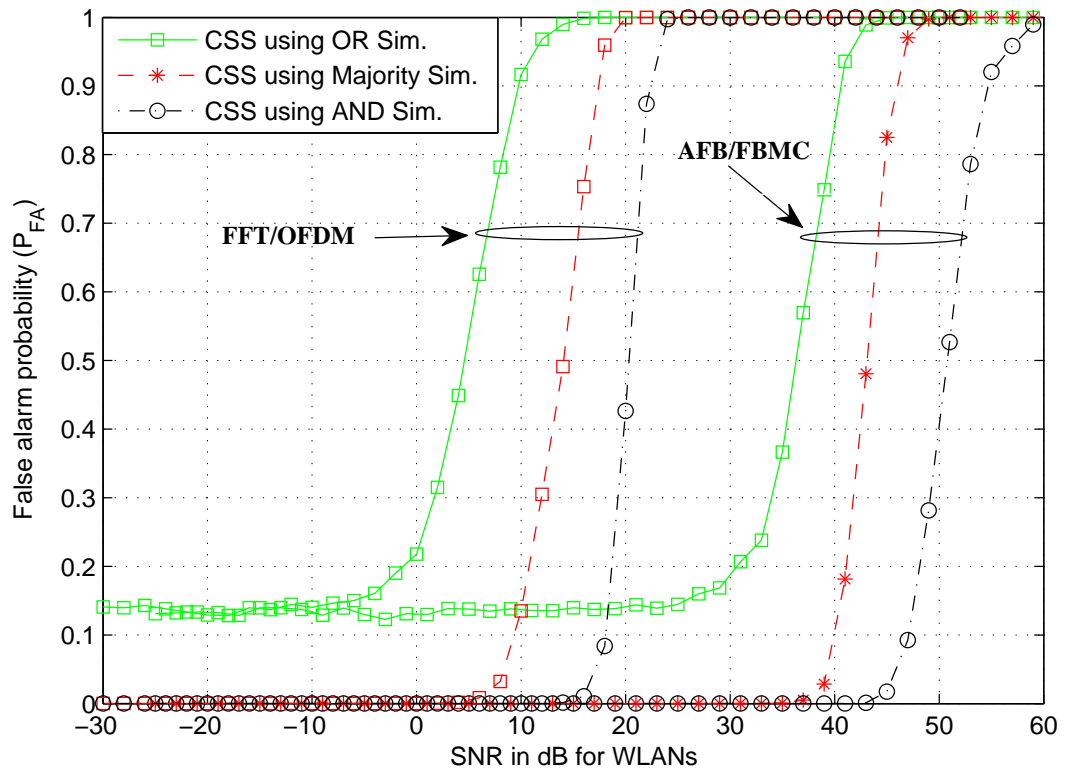


Figure 4.6: Comparison of CSS false alarm probabilities between FFT processing of OFDM based PU and AFB processing of FBMC based PU with three different linear fusion rules under ideal mode (no PA effects) for $N_{FFT} = 250$, the time record length $N_t = 50$, the frequency block length $N_f = 5$, and the number of sensing stations $M = 8$.

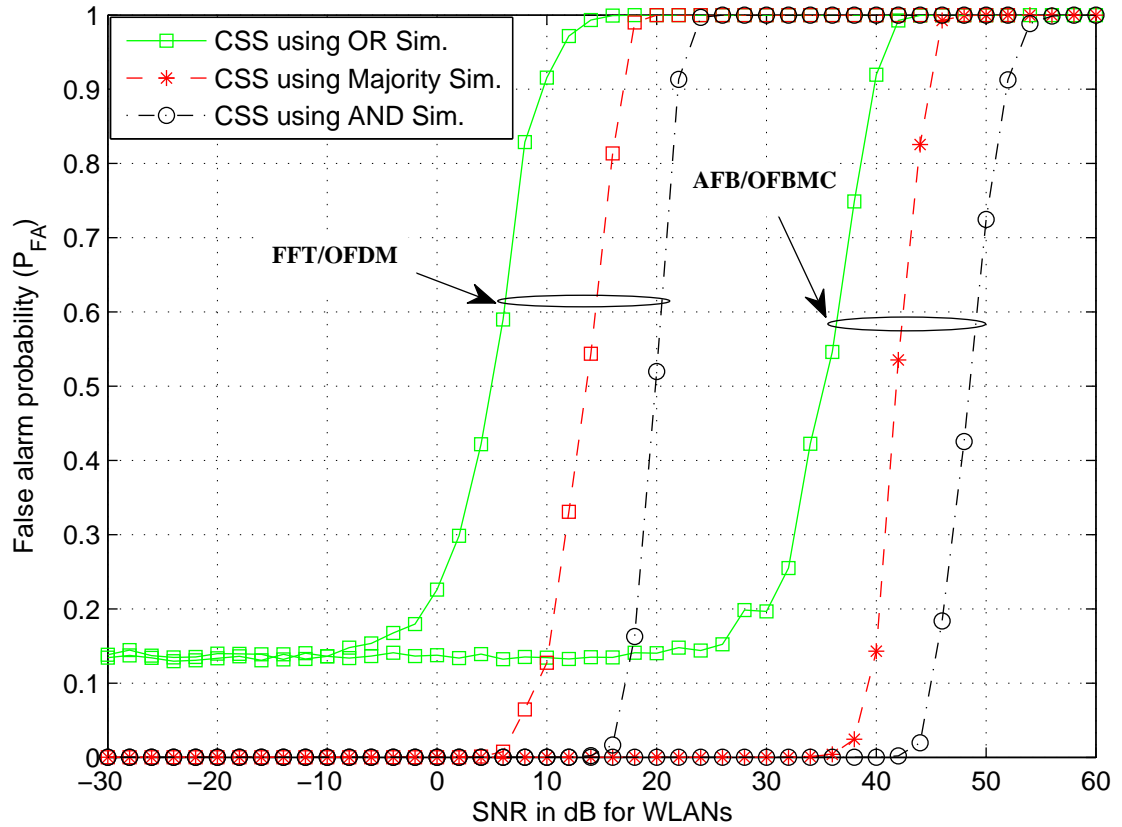


Figure 4.7: Comparison of CSS false alarm probabilities between FFT processing of OFDM based PU and AFB processing of FBMC based PU with three different linear fusion rules under power amplifier effects for $N_{FFT} = 250$, the time record length $N_t = 50$, the frequency block length $N_f = 5$, and the number of sensing stations $M = 8$.

Both ideal and practical power amplifier cases have been considered in these studies. Results from both ideal and practical power amplifier case have been depicted in Figure 4.6 and 4.7, respectively. With linear power amplifier, the interference from the PU signals is low and the spectral hole is wider. Since 802.11g like FBMC based WLAN signal model shows the best performance as FBMC has the better spectral containment compared to OFDM based WLAN. AFB processing of FBMC based WLAN shows significant enhancement over FFT processing of OFDM based WLAN model. "OR rule" shows higher false alarm probabilities compared to other fusion rules. On the other hand, "AND rule" shows lowest false alarm and "Majority rule" shows moderate false alarm probabilities for fixed set of SNR values.

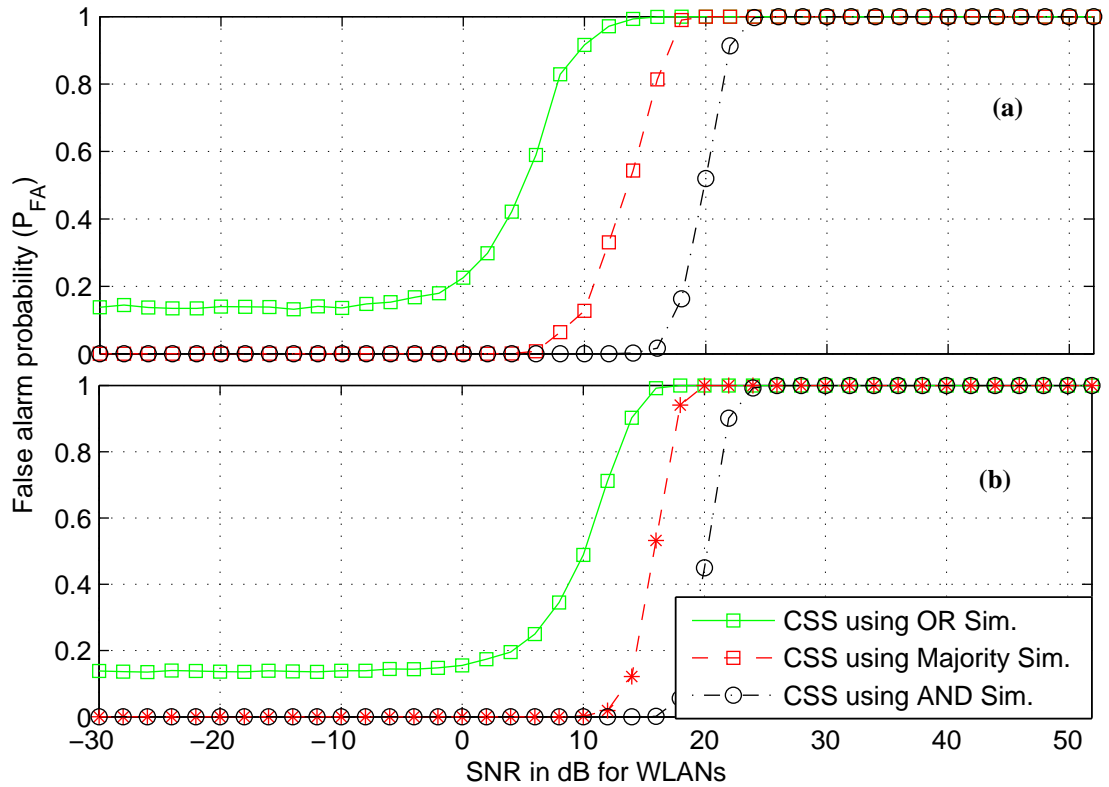


Figure 4.8: CSS false alarm probabilities for FFT processing of a) OFDM and b) FBMC based PU with three different linear fusion rules under power amplifier effects for the number of FFT length is $N_{FFT} = 250$, the time record length $N_t = 50$, the frequency block length $N_f = 5$, and the number of sensing stations $M = 8$.

FFT processing of FBMC can also be possible and simulation results have been compared with the FFT processing of OFDM as in Figure 4.8. FFT processing of FBMC shows better results compared to FFT processing of OFDM. However, AFB processing of FBMC has optimum performance compared to all other techniques.

4.5 Chapter Summary

In this chapter, subband based CSS was presented. FFT and AFB processing of wide-band multicarrier based PU model were proposed to investigate spectral hole between two 802.11g standard OFDM and 802.11g like FBMC based WLAN signals. Effects of an interference on the spectral gap was investigated. FBMC based multicarrier with better spectral containment showed the optimum performance compare to OFDM based multicarrier. Proposed AFB based CSS methods with FBMC based PU model, outperformed other sensing methods. It fitted well even for CR system with narrow spectral gap. Interference in SU band was also modeled in this study. In simulation results, AFB processing of 802.11g like FBMC based WLAN signal showed the optimum performance.

5. MAXIMUM-MINIMUM SUBBAND ENERGY BASED COOPERATIVE SPECTRUM SENSING

In this chapter, the novel maximum-minimum energy detection based CSS method is proposed. This sensing technique is robust to the noise uncertainty and yet reduces the complexity in comparison to existing methods with such robustness. The proposed sensing techniques outperform the other advance spectrum sensing methods under noise uncertainty condition. Specifically, the chapter contributes to the following issues:

- Novel spectrum sensing techniques are proposed and they are simpler to implement, including robust to noise uncertainty.
- Number of CR receivers are proposed to make the collaborative decision so as to enhance the detection performance and to counteract the practical wireless channel effects.
- A novel analytical method is proposed and the results are compared to simulations.
- Novel Max-Min ED based CSS is proposed with improved performance over traditional CSS.

Section 5.1 gives a brief overview of the Max-Min ED based proposed CSS which is described in more details in Section 5.2. Section 5.3 presents the analytical model for cooperative Max-Min ED based spectrum sensing. Section 5.4 presents the analysis of the results obtained from the computer based simulation. Comparison of the results with other spectrum sensing techniques is presented in the same section. At last, conclusions are presented.

5.1 Introduction

A matter of primary interest is to design algorithms that can deliver acceptable spectrum sensing performance with reduced complexity and reliability in terms of detection and false alarm performance. Existing spectrum sensing techniques are not satisfying in this respect. Particularly, sensing in low SNR range, i.e. (-25 dB, -10 dB) is challenging due to the noise susceptibility issues and the hidden node problem also exists. To counteract these issue, the spectrum sensing technique has to be more robust to noise uncertainty, while exhibiting realistic computational complexity for practical implementation. This

study is motivated to solve the problem of complexity and noise uncertainty. In this chapter, novel cooperative Max-Min ED scheme is proposed which reduces complexity and noise uncertainty. Literature in [18] covers the idea of the frequency diversity gain exploitation with the help of the statistics of the energy spectral density (ESD). Differential stage is suggested in the literature as a solution to the noise uncertainty. However, studies in our group have proposed a solution without the differential stage, while maintaining the robustness to noise and reduced computational complexity. Results show that the proposed solution outperform the performances the traditional ED and other detection algorithms. Figure 5.1 shows the steps implemented in Max-Min ED algorithm.

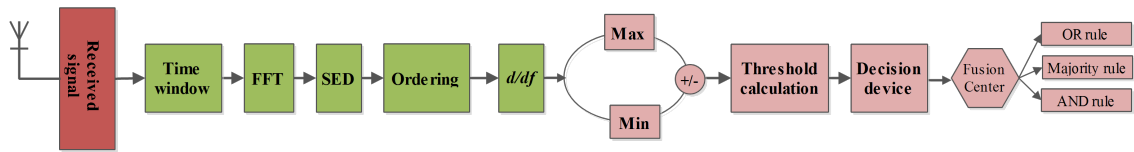


Figure 5.1: Block diagram of Max-Min ED based CSS method.

5.2 Proposed Max-Min ED based CSS Method

In this section, a novel Max-Min ED method is considered, which is less complex than existing methods which are robust to noise uncertainty. Illustration of the methods is in Figure 5.1. The maximum and minimum energies of the subbands are utilized for constructing the decision statistics. These statistics are used to estimate the presence and absence of PU. Actually, we consider here three alternative schemes, which are utilizing the subband energies in a different manner [15]. These methods consists of following steps:

- SED to calculate subband energies,
- Ordering of the determined subband energies,
- Differentiation of the ordered subband energy sequence,
- Quantification of the maximum and minimum energies level,
- Calculation of a threshold and the implementation of decision device.

The proposed method removes the ordering and differentiation blocks from the Figure 5.1. Hence, the proposed method is less complex yet outperforms the other sensing methods.

5.2.1 Subband Energy Detector

The FFT operation on blocks of N_{FFT} input samples is applied. Alternatively, AFB with N_{FFT} subbands can be used and this choice is preferred in high dynamic range scenarios. The subband signals are formulated as in Equation 2.8. Frequency variability of an ESD process is featured in Max-Min ED algorithms as depicted in the Figure 5.1 and the process is summarize as, $U_k = \frac{1}{L_t} \sum_{m=1}^{L_t} |Y_k[m]|^2$, where $L_t = N/N_{FFT}$ represents length of the window. From the central limit theorem, U_k for both \mathcal{H}_0 and \mathcal{H}_1 hypotheses is expressed as,

$$U_k = \begin{cases} \mathcal{N}(\sigma_{w,k}^2, \frac{2}{L_t} \sigma_{w,k}^4), & \mathcal{H}_0 \\ \mathcal{N}\left(|H_k|^2 \sigma_k^2 + \sigma_{w,k}^2, \frac{2}{L_t} (|H_k|^2 \sigma_k^2 + \sigma_{w,k}^2)^2\right). & \mathcal{H}_1 \end{cases} \quad (5.1)$$

Maximum and minimum energies are estimated as depicted in Figure 5.1 and the test statistics is calculated from the energy values. Test statistic is then compared with a predetermined threshold that is obtained from the target P_{FA} with the aid of Gumbel distribution. Presence and absence status of the PU signal is determined by comparing the threshold and test statistics. Analytical approach to calculate the thresholds will be given later in Section 5.3 [15] [18].

5.2.2 Cooperative Maximum-Minimum Energy Detection

The proposed cooperative Max-Min ED uses the linear fusion rules at the FC to combine the sensing results from each sensing station, each of which applies the Max-Min ED. A number of CR receivers is used for collaboration to estimate the presence of PU signal in more reliable manner. Our study assumes 8 cooperating CRs. Linear fusion rules are applied to estimate cooperative detection and false alarm probabilities. Different detection probabilities are achieved at FC depending on the fusion rule applied. Similarly, false alarm probability varies in accordance to the fusion rule applied at the FC. Both, cooperative detection and false alarm probabilities are calculated as follows,

$$P_{D,t} : \begin{cases} = 1 - (1 - P_D)^M & \text{"OR rule"} \\ = P_D^M & \text{"AND rule"} \\ = \sum_{j=M/2}^M \binom{M}{j} P_D^j (1 - P_D)^{M-j} & \text{"Majority rule"} \end{cases} \quad (5.2)$$

$$P_{FA,t} : \begin{cases} = 1 - (1 - P_{FA})^M & \text{"OR rule"} \\ = P_{FA}^M & \text{"AND rule"} \\ = \sum_{j=M/2}^M \binom{M}{j} P_{FA}^j (1 - P_{FA})^{M-j} & \text{"Majority rule"} \end{cases} \quad (5.3)$$

Here $P_{D,t}$ and $P_{FA,t}$ are the detection and false alarm probabilities, respectively under CSS. P_D and P_{FA} are detection and false alarm probabilities of the individual CR user, respectively.

5.3 Analytical Models for Max-Min based Energy Detector

In this section, novel analytic expressions for the Max-Min ED based CSS are formulated. Later, the derived analytical results are compared to simulation results, and a very good match is found between them [18].

5.3.1 Probability of False Alarm and Energy Threshold

Recalling earlier studies, the test statistics depend on the maximum and minimum values of U_k . The statistics of maximum and minimum distribution is characterized by the Von Mises theorem [18]. Following these statistics, the Gumbel distribution [15] is used for efficient representation of the extreme values of an arbitrary distribution namely,

$$f_{min}(x) = \frac{1}{\beta} e^{\frac{x-\alpha}{\beta}} e^{-e^{\frac{x-\alpha}{\beta}}} \quad (5.4)$$

and,

$$f_{max}(x) = \frac{1}{\beta} e^{-\frac{x-\alpha}{\beta}} e^{-e^{-\frac{x-\alpha}{\beta}}} \quad (5.5)$$

here α and β represent the location and scale parameters of the distribution. The expected value and standard deviation of the difference of maximum and minimum values are derived from the equations 5.4 and 5.5, respectively. Based on the above equation and earlier studies of our group [15] both detection and false alarm probabilities for each sensing station are formulated as Equations 5.9 and 5.7, respectively.

Using Gumbel distribution with mean and variance, values of U_k in 5.1 for hypothesis \mathcal{H}_0 , one obtains

$$\begin{aligned} U_{max-min} | \mathcal{H}_0 &\sim \mathcal{QG}(\alpha | \mathcal{H}_0, \beta | \mathcal{H}_0) \\ &\sim \mathcal{QG}\left(\frac{\sigma_{w,k}^2}{2} + C \sqrt{\frac{6}{L_t}} \frac{\sigma_{w,k}^2}{\pi}, \sqrt{\frac{6}{L_t}} \frac{\sigma_{w,k}^2}{\pi}\right) \end{aligned} \quad (5.6)$$

here, $\mathcal{QG}(\alpha, \beta)$ denotes the Gumbel distribution, and standard complementary function is

represented by, $\mathcal{G}\left(\frac{x-\alpha}{\beta}\right) = 1 - e^{-e^{-\frac{x-\alpha}{\beta}}}$.

In the practical environment, both expressions P_{FA} and P_D have to consider the noise uncertainty. It is recalled that the noise distribution is summarized in the range by $\sigma_{w,k}^2 \in [\frac{1}{\rho}\sigma_{n,k}^2, \rho\sigma_{n,k}^2]$ where ρ is the corresponding noise uncertainty parameter. Hence, the worst-case false alarm probability is expressed as follows:

$$\begin{aligned} P_{FA} &= \max_{\sigma_{w,k}^2 \in [\frac{1}{\rho}\sigma_{n,k}^2, \rho\sigma_{n,k}^2]} \mathcal{G}\left(\frac{\gamma - \left(\frac{\sigma_{w,k}^2}{2} + C\sqrt{\frac{6}{L_t}}\frac{\sigma_{w,k}^2}{\pi}\right)}{\left(\frac{6}{L_t}\right)^{1/4}\frac{\sigma_{w,k}}{\sqrt{\pi}}}\right) \\ &= \mathcal{G}\left(\frac{\gamma - \left(\frac{\rho\sigma_{n,k}^2}{2} + C\sqrt{\frac{6}{L_t}}\frac{\rho\sigma_{n,k}^2}{\pi}\right)}{\left(\frac{6}{L_t}\right)^{1/4}\sqrt{\frac{\rho}{\pi}}\sigma_{n,k}}\right). \end{aligned} \quad (5.7)$$

here, ρ is corresponding uncertainty parameter, Based on 5.7 threshold is formulated as,

$$\gamma = \mathcal{G}^{-1}(P_{FA}) \left(\frac{6}{L_t}\right)^{1/4} \sqrt{\frac{\rho}{\pi}}\sigma_{n,k} + \frac{\rho\sigma_{n,k}^2}{2} + C\sqrt{\frac{6}{L_t}}\frac{\rho\sigma_{n,k}^2}{\pi}. \quad (5.8)$$

5.3.2 Probability of Detection

Similarly, detection probability is derived for \mathcal{H}_1 hypothesis from the equation 5.1 as follows,

$$\begin{aligned} P_D &= \min_{\sigma_{w,k}^2 \in [\frac{1}{\rho}\sigma_{n,k}^2, \rho\sigma_{n,k}^2]} \mathcal{G}\left(\frac{\gamma - \left(\frac{\kappa}{2} + C\sqrt{\frac{6}{L_t}}\frac{\kappa}{\pi}\right)}{\left(\frac{6}{L_t}\right)^{1/4}\frac{\kappa}{\sqrt{\pi}}}\right) \\ &= \mathcal{G}\left(\frac{\gamma - \left(\frac{\hat{\kappa}}{2} + C\sqrt{\frac{6}{L_t}}\frac{\hat{\kappa}}{\pi}\right)}{\left(\frac{6}{L_t}\right)^{1/4}\sqrt{\frac{\rho}{\pi}}\hat{\kappa}}\right). \end{aligned} \quad (5.9)$$

here $\kappa = E_{max} - E_{min} + \sigma_{w,k}^2$ and $\hat{\kappa} = E_{Max} - E_{Min} + \sigma_{n,k}^2/\rho$. E_{max} and E_{min} are evaluated as $E_{max} = \max_k(|H_k|^2 H_k)$ and $E_{min} = \min_k(|H_k|^2 E_k)$. H_k and E_k are PU channel gain and PU signal energy in subband k .

Noise uncertainty introduces severe effects in ED based spectrum sensing methods. The proposed method efficiently removes the noise floor. Since the observed primary signal power spectral density (PSD) is frequency dependent and the noise is additive white Gaussian noise, the proposed maximum-minimum approach eliminates the noise floor. Removal of the noise floor minimizes the uncertainty effects and hence the proposed Max-Min based CSS method is robust is to noise uncertainty.

5.3.3 Analysis of Cooperative Maximum-Minimum Energy Detection

Analytical detection and false alarm probabilities with Max-Min ED are obtained from the Equations 5.9 and 5.7, respectively. Linear fusion rules are applied to combine the sensing results from the each station. Here, linear fusion rules for hard decision combining are applied at FC using "AND rule", "OR rule" and "Majority rule". Details of these linear fusion rules have been covered in Section 3.3.

From Equations 5.9 and 5.7, P_D and P_{FA} for individual sensing station with Max-Min ED is calculated. Cooperative probabilities after implementation of linear fusion rules are obtained from the different fusion rules as per Equation 5.2 and 5.3, respectively.

5.4 Simulation Results

The performance of proposed novel Max-Min ED based CSS and the comparison with traditional ED based CSS are shown in this section. Proposed Max-Min ED based CSS methods are realized for non-oversampled, small-oversampled and 2x-oversampled signal cases. In our test scenario, proposed CSS are analyzed with different channel models: Indoor, ITU-R and SUI-1 frequency selective channels [30]. With worst-case scenario of 1-dB noise uncertainty, desired false alarm probability is chosen as $P_{FA} = 0.01$ for each station in all cases. The time record length is 10240 samples is selected. 1000 Monte Carlo simulations applied to ensure the reliability of the simulation. In this study, two FFT length were set as $N_{FFT} = 8,32$. Number of sensing stations $M = 8$ was selected. System bandwidth for the test scenario was set to 20 MHz.

Three different approaches, maximum-minimum ED, maximum/minimum ED and differential Max-Min ED based CSS approach have been presented in Figure 5.2 - 5.5. Cooperative Max-Min ED based algorithm has better performance over the differential Max-Min ED and Max/Min ED based algorithms. Hence, cooperative Max-Min ED is proposed for the spectrum sensing purposes. Furthermore, the algorithm is simpler to implement and yet eliminates the noise floor thus reduces the uncertainty effects. CSS offers the reliability and the solution to the potential hidden node problem as described in the earlier chapter.

5.4.1 Comparison of Max-Min ED, Max/Min ED, and differential Max-Min ED based CSS

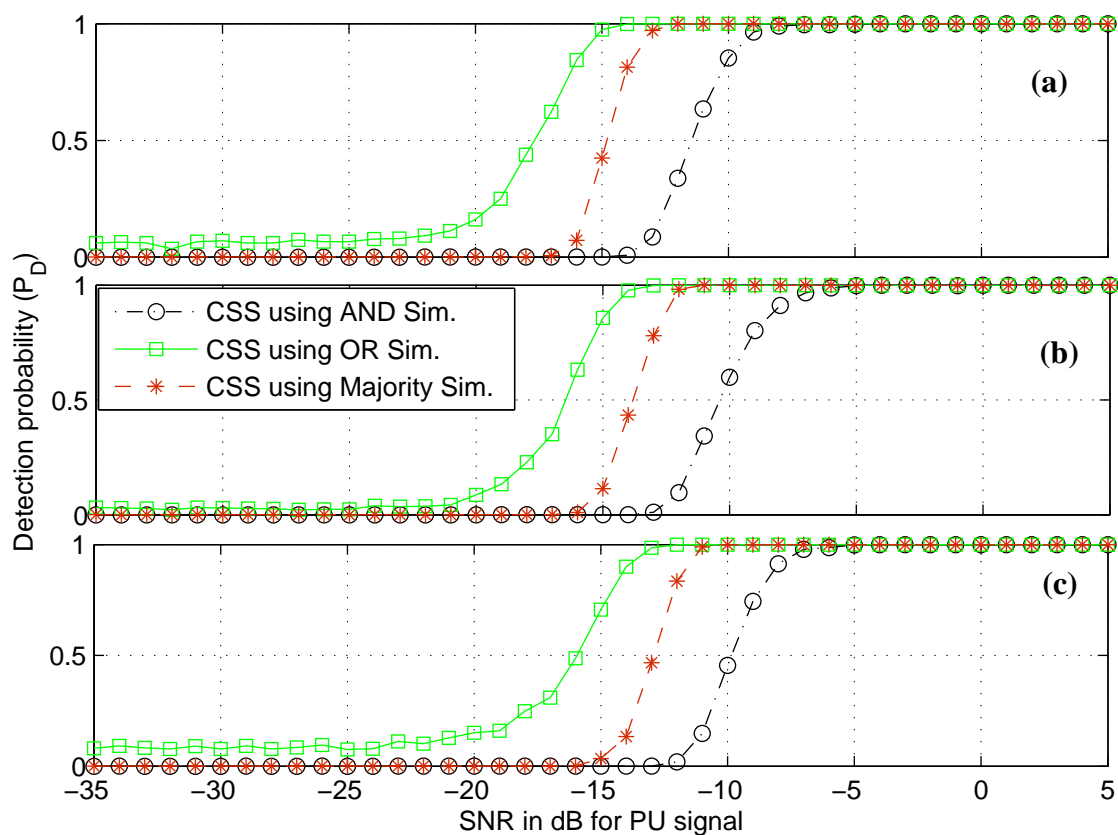


Figure 5.2: CSS detection probabilities with a) Max-Min ED, b) Max/Min ED and c) Diff. Max-Min ED and three different linear fusion rules for non-oversampled QPSK PU signal under Indoor channel, the length of FFT $N_{FFT} = 8$, the number of sensing stations $M = 8$, the sample complexity $N = 10240$, and 1 dB noise uncertainty.

Figure 5.2 gives the comparison between proposed novel Max-Min ED, Max/Min ED, and differential Max-Min ED with three different linear fusion rules. Detection probabilities of three different techniques were compared for frequency selective Indoor channel. Length of FFT is selected $N_{FFT} = 8$, the number of sample complexity is equals to $N = 10240$ for non-oversampled QPSK PU signal. Figure shows Max-Min ED with better detection probabilities compared to Max/Min ED, and differential Max-Min ED based CSS.

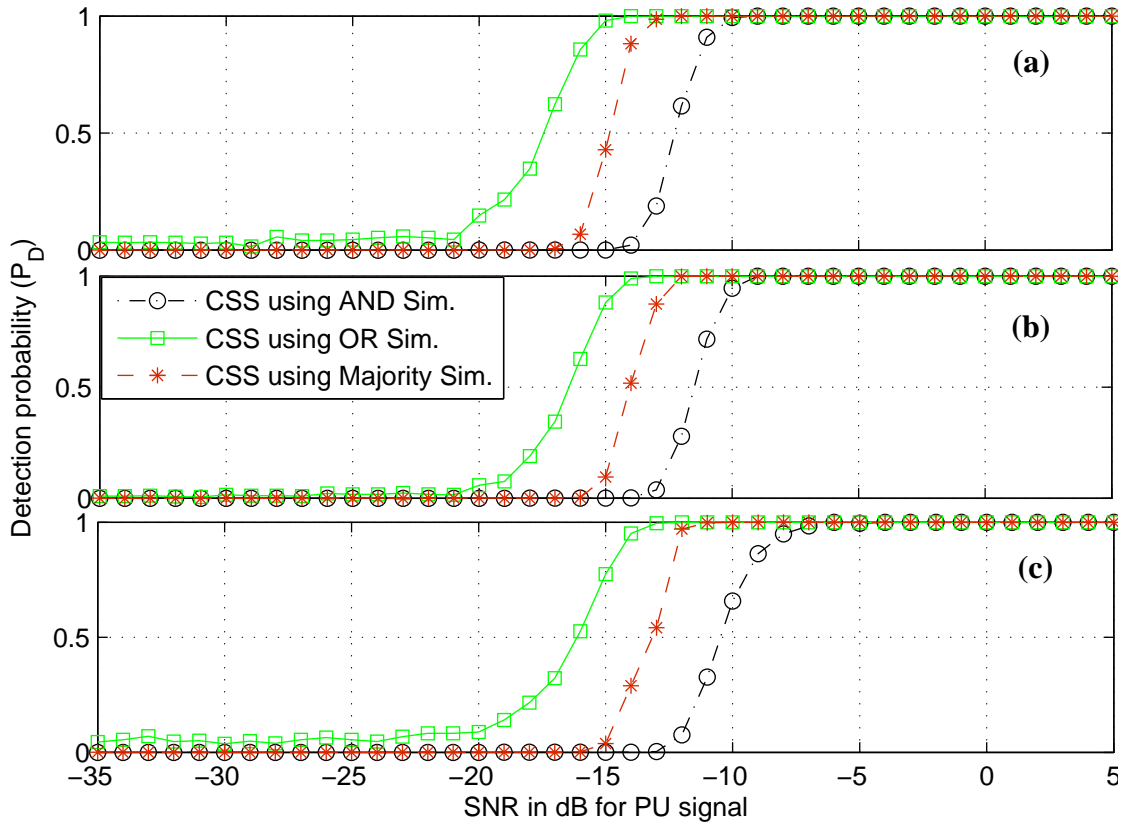


Figure 5.3: CSS detection probabilities with a) Max-Min ED, b) Max/Min ED and c) Diff. Max-Min ED and three different linear fusion rules for small-oversampled QPSK PU signal under Indoor channel, the length of FFT $N_{FFT} = 8$, number of sensing stations $M = 8$, the sample complexity $N = 10240$, and 1 dB noise uncertainty

Figure 5.3 gives the comparison between proposed novel Max-Min ED, Max/Min ED, and differential Max-Min ED with three different linear fusion rules. Detection probabilities of three different techniques were compared for frequency selective Indoor channel. Length of FFT is selected $N_{FFT} = 8$. With small oversampling, the number of sample complexity is equals to $N = 12480$ for QPSK PU signal. Here, small oversampling is selected to cover the transition band near the signal spectra. Figure shows Max-Min ED with better detection probabilities compared to Max/Min ED, and differential Max-Min ED based CSS.

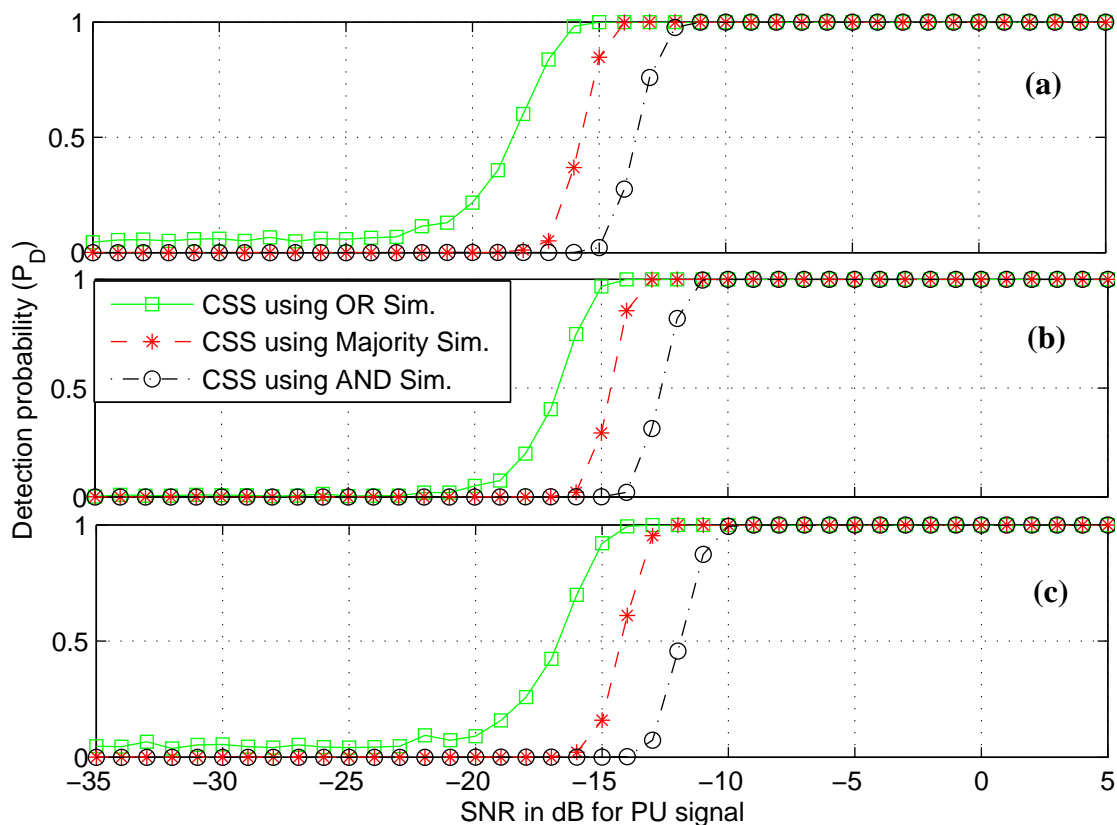


Figure 5.4: CSS detection probabilities with a) Max-Min ED, b) Max/Min ED and c) Diff. Max-Min ED and three different linear fusion rules for 2x-oversampled QPSK PU signal under Indoor channel, the length of FFT $N_{FFT} = 8$, number of sensing stations $M = 8$, the sample complexity $N = 10240$, and 1 dB noise uncertainty.

Figure 5.4 gives the comparison between proposed novel Max-Min ED, Max/Min ED, and differential Max-Min ED with three different linear fusion rules. Detection probabilities of three different techniques were compared for frequency selective Indoor channel. Length of FFT is selected $N_{FFT} = 8$ for QPSK PU signal. Here, 2x-oversampling is selected with root raised cosine filter and 22% roll off factor. Figure shows Max-Min ED with better detection probabilities compared to Max/Min ED, and differential Max-Min ED based CSS.

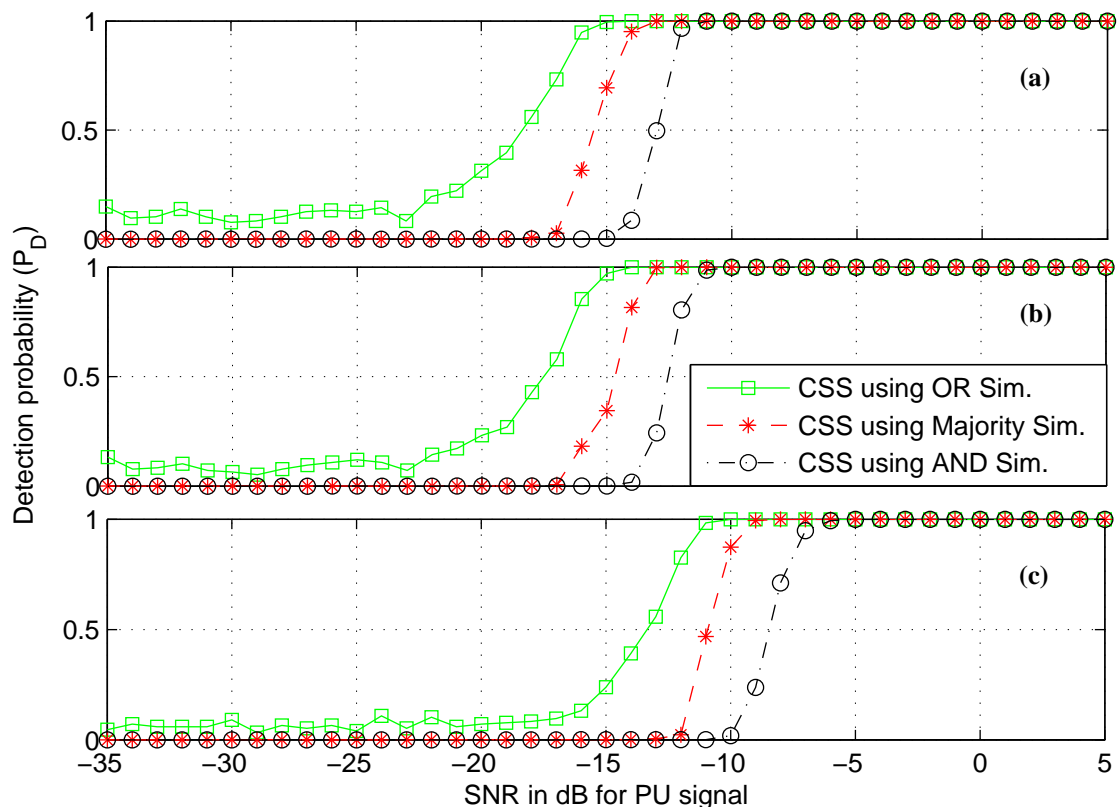


Figure 5.5: CSS detection probabilities with a) Max-Min ED, b) Max/Min ED and c) Diff. Max-Min ED and three different linear fusion rules for 2x-oversampled QPSK PU signal under Indoor channel, the length of FFT $N_{FFT} = 32$, the number of sensing stations $M = 8$, the sample complexity $N = 10240$, and 1 dB noise uncertainty.

Here, number of FFT length is selected as $N_{FFT} = 32$ in Figure 5.5. Max-Min ED shows better detection probabilities compared to Max/Min ED, and differential Max-Min ED based CSS.

Novel Max-Min ED based CSS shows better detection probabilities compared to Max/Min ED, and differential Max-Min ED based CSS in all non-oversampled, small-oversampled and 2x-oversampled signal cases for $N_{FFT} = 8, 32$.

5.4.2 Comparison of Analytical and Simulated Results of Max-Min ED and Traditional Cooperative ED

Proposed cooperative Max-Min ED have been compared with the traditional cooperative ED under 1 dB noise uncertainty condition. Simulations have been carried out for $N_{FFT} = 8$ and 32 as portrayed by Figures 5.6 and 5.7 respectively. Both figures show that proposed cooperative Max-Min ED clearly edge the performances of traditional cooperative ED. Additionally, analytical results of proposed cooperative Max-Min ED have been compared with simulation results. Results in both Figures 5.6 and 5.7 match quite

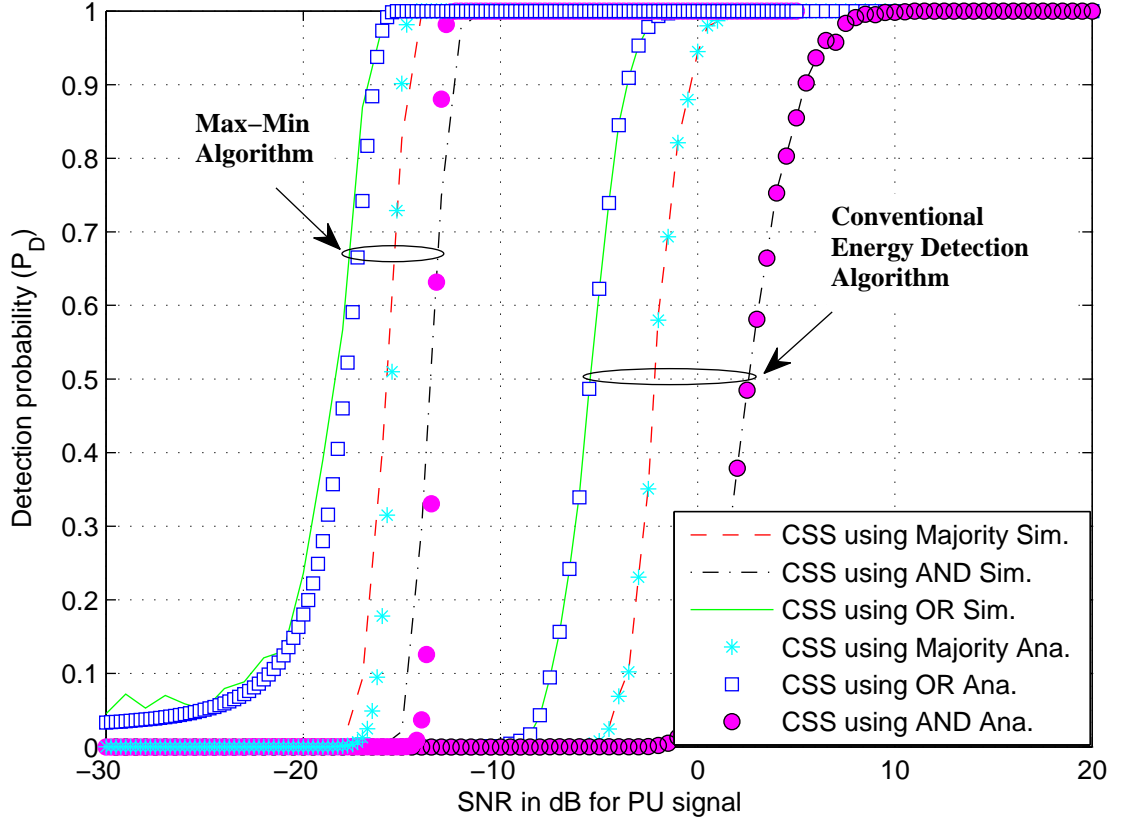


Figure 5.6: Comparison of CSS detection probabilities between traditional ED and Max-Min ED with three different linear fusion rules for 2x-oversampled QPSK PU signal under Indoor channel model, the length of FFT $N_{FFT} = 8$, the number of sensing stations $M = 8$, the sample complexity $N = 10240$, and 1 dB noise uncertainty.

well. Proposed cooperative Max-Min ED has approximately 10 dB better detection performance compared to traditional cooperative ED under 1 dB noise uncertainty condition. Few spikes have been observed in the simulation results for the "OR rule", number of Monte-Carlo simulation is increased to minimize the spikes. "Majority rule" has moderate value of both detection and false alarm probabilities. Hence, "Majority rule" with $k=M/2$ is proposed for the collaborative decision fusion. Additionally, results show that the proposed Max-Min ED is better than that of conventional ED algorithms for both number of subband 8 and 32.

Figure 5.6 shows the detection probabilities for traditional ED and Max-Min ED with three different linear fusion rules applied at the FC. Length of FFT is selected to $N_{FFT} = 8$. 2x-oversampled QPSK signal was selected with 1-dB noise uncertainty. Frequency selective Indoor channel with AWGN noise is selected. On comparison Max-Min ED with three different fusion rules shows better performance over traditional ED with three different fusion rules. For Max-Min ED, 90 % detection probabilities for "OR rule", "Majority rule", and "AND rule" is achieved at -16 dB, -14 dB and -12 dB, respectively. On other hand, traditional ED shows 90 % detection probabilities for "OR rule", "Majority

rule", and "AND rule" are achieved at -4 dB, 0 dB and 5 dB, respectively. Figure shows the $P_{FA,t}$ for "OR rule" is higher compare to "Majority rule" and "AND rule".

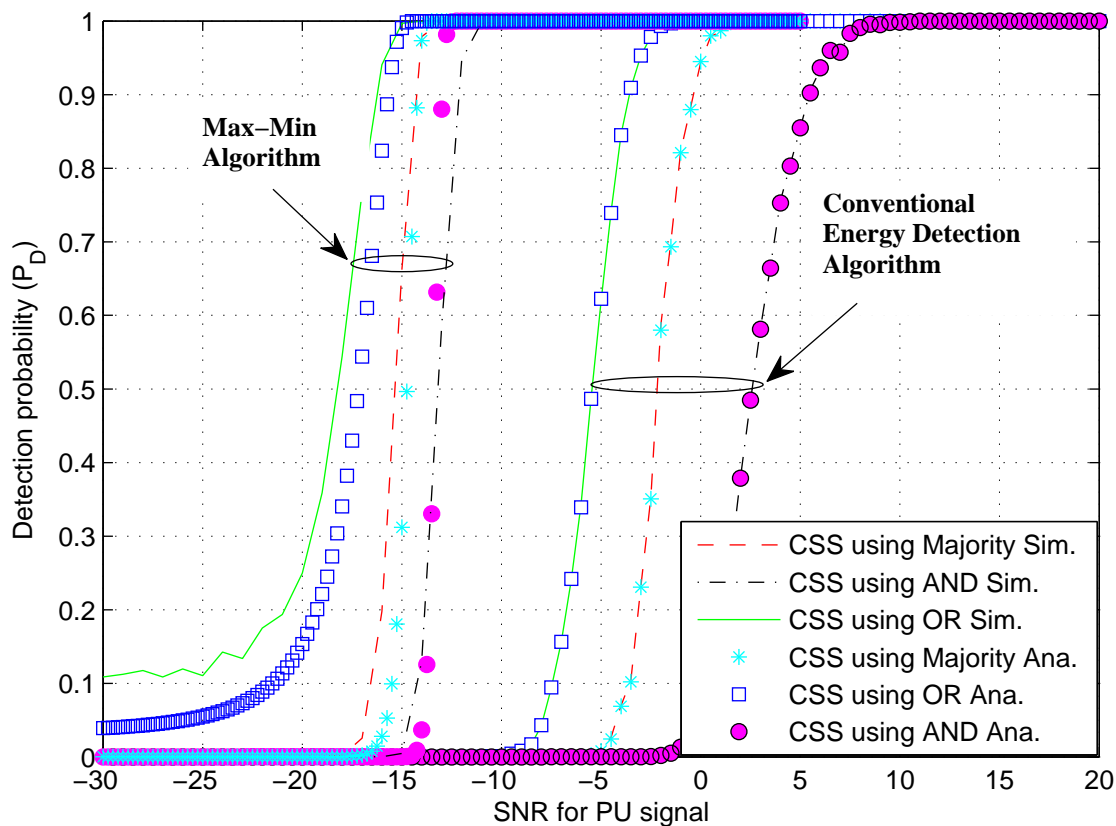


Figure 5.7: Comparison of detection probabilities between traditional ED and Max-Min ED with three different linear fusion rules for 2x-oversampled QPSK PU signal under Indoor channel model, the length of FFT $N_{FFT} = 32$, the number of sensing stations $M = 8$, and the number of sampling complexity $N = 10240$, and 1 dB noise uncertainty.

Figure 5.7 shows the detection probabilities for traditional ED and Max-Min ED with three different linear fusion rules applied at the FC. Length of FFT is selected to $N_{FFT} = 32$. 2x-oversampled QPSK PU signal was selected with 1-dB noise uncertainty. Max-Min ED shows 90 % detection probabilities for "OR rule", "Majority rule", and "AND rule" are achieved at -15 dB, -13 dB and -12 dB, respectively. On other hand, traditional ED shows 90 % detection probabilities for "OR rule", "Majority rule", and "AND rule" are achieved at -4 dB, 0 dB and 5 dB, respectively.

Figure 5.8 and 5.9 show comparison of ROC curves with both Max-Min ED and traditional α ed based CSS with three different linear fusion rules. In test scenario, number of sensing stations are selected $M = 8$, the number of sample complexity is selected $N = 10240$. 2x-oversampled PU signal with noise uncertainty parameter equals to 0, 0.1 and 1 dB are selected. Result shows that even with small noise uncertainty traditional ED performances decreases significantly. On other hand, proposed novel Max-Min ED based

CSS are immune to the noise uncertainty.

ROC curves for the proposed Max-Min ED and the traditional ED with/without noise uncertainty under -16 dB SNR value are shown in Figure 5.8 -5.9. These results reflect a fundamental tradeoff between P_{FA} and P_D . Small noise uncertainty, such as 0.1 dB effects the detection performance significantly in the traditional ED, whereas the proposed Max-Min ED based approach provides robust detection performance even under high noise uncertainty values, such as 1 dB.

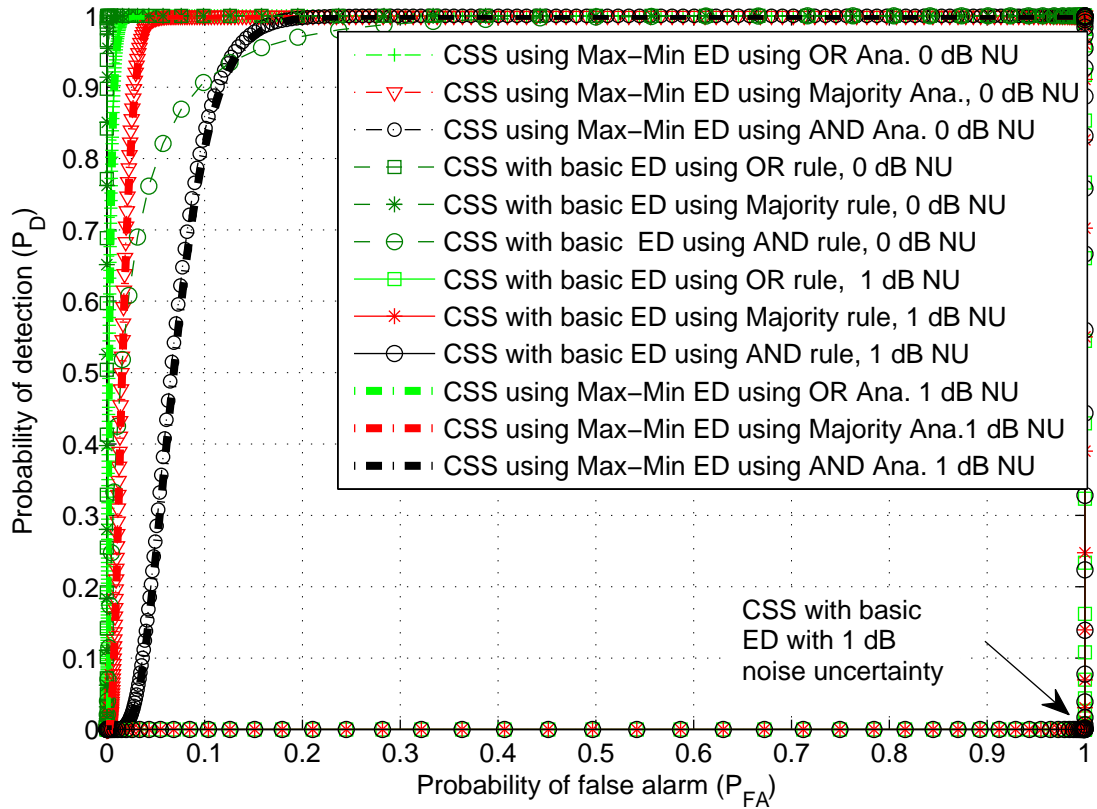


Figure 5.8: Comparison of CSS ROC curve with both basic ED and Max-Min ED and three different fusion rules at $\gamma = -14$ dB for 2x-oversampled PU signal without frequency selective channel and fading effects, the number of sensing stations $M = 8$, the length of FFT $N_{FFT} = 8$, and the sample complexity $N = 10240$.

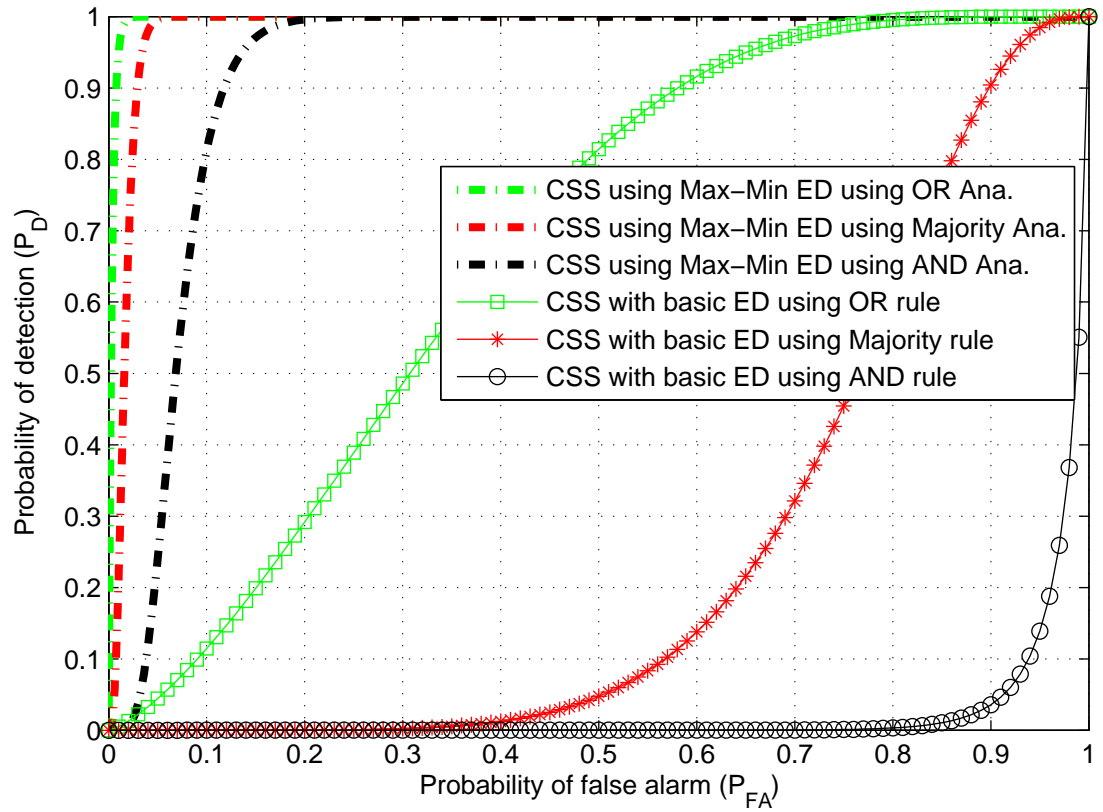


Figure 5.9: Comparison of CSS ROC curve with both basic ED and Max-Min ED and three different fusion rules at $\gamma = -14$ dB for 2x-oversampled PU signal without frequency selective channel and fading effects, the number of sensing stations $M = 8$, the length of FFT $N_{FFT} = 8$, the sample complexity $N = 10240$, and 0.1 dB noise uncertainty.

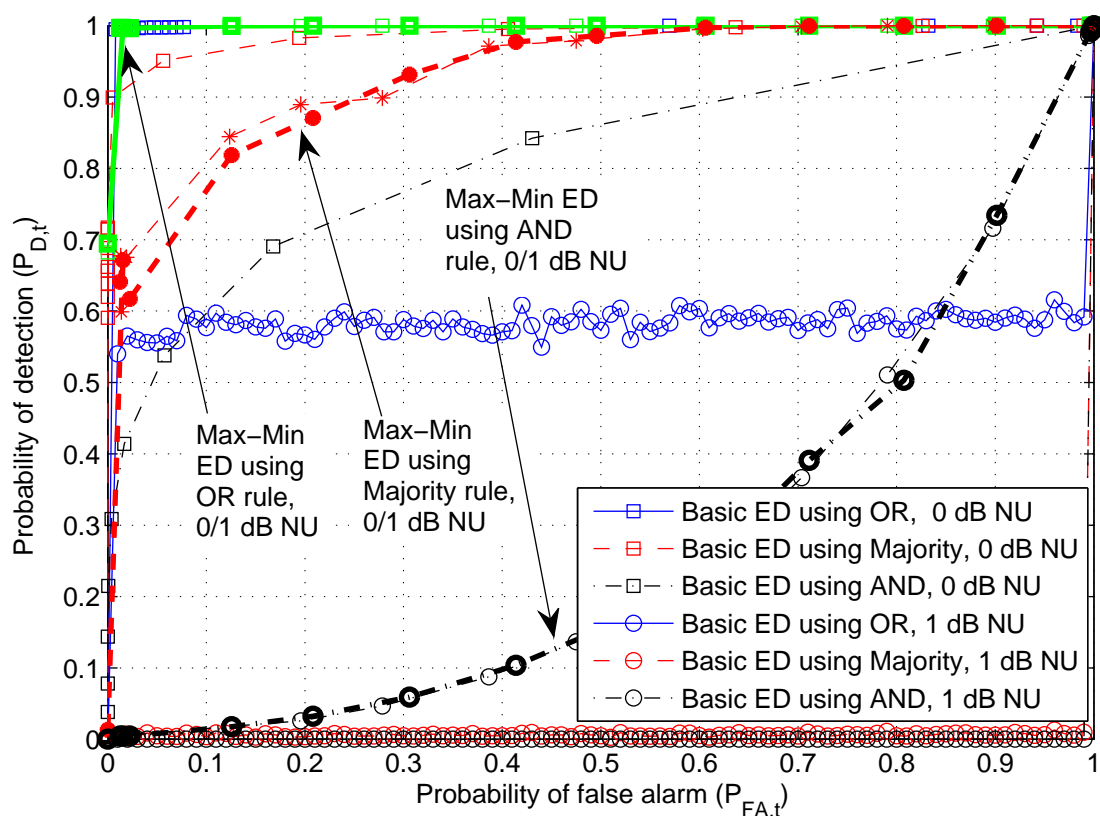


Figure 5.10: Comparison of CSS ROC curve with both basic ED and Max-Min ED and three different fusion rules at $\gamma = -14$ dB for $2x$ -oversampled PU signal, the channel model is SUI-I with frequency flat lognormal fading with standard deviation 9 dB, the number of sensing stations $M = 8$, the length of FFT $N_{FFT} = 8$, the sample complexity $N = 10240$, and noise uncertainty parameter [0,1] dB.

ROC curves for CSS based on both Max-Min ED and basic ED are simulated and compared in Figure 5.10 for $\gamma = -14$ dB and noise uncertainty parameter [0,1] dB. SUI-I channel with frequency-flat lognormal fading with standard deviation of 9 dB is considered. Figure shows, Max-Min ED algorithms is immune to the noise uncertainty even on high noise uncertainty, like 1 dB. However, performance of the basic ED based CSS algorithm is decreases significantly even with small noise uncertainty, like 0.1 dB . Figure 5.11 shows performance of basic ED based CSS algorithm is decreases significantly under 0.1 dB noise uncertainty.

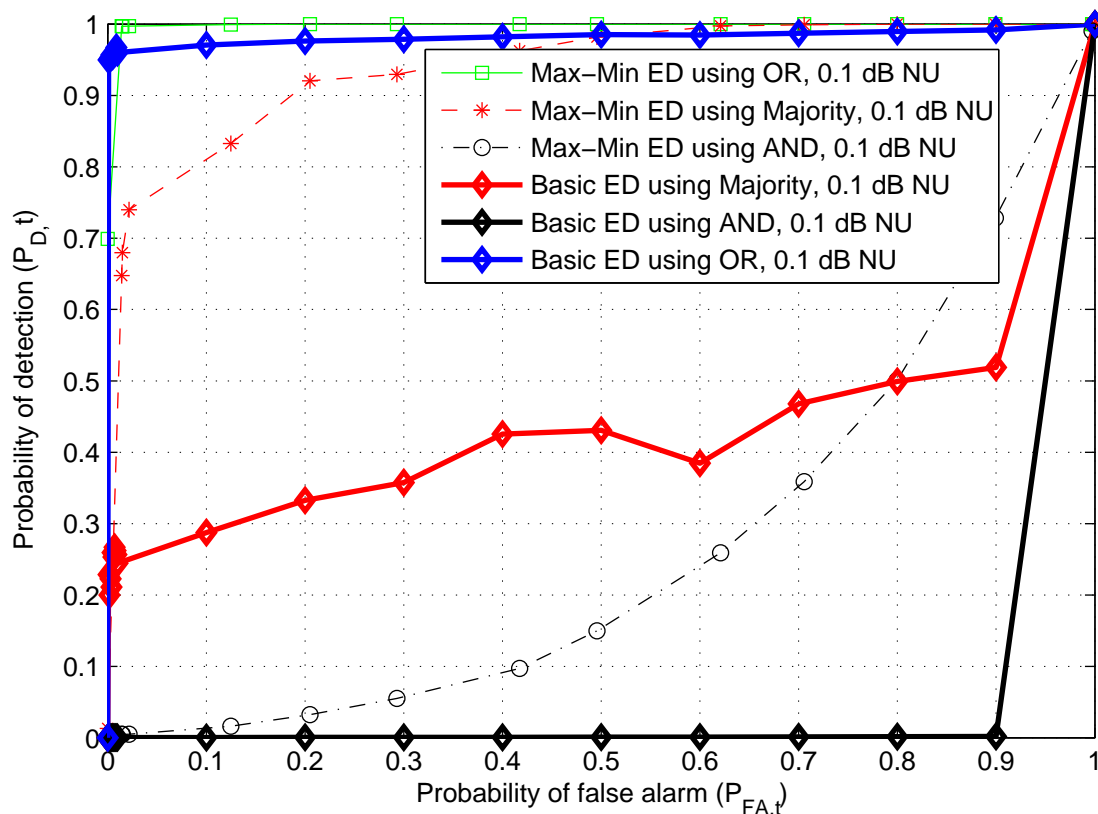


Figure 5.11: Comparison of CSS ROC curve with both basic ED and Max-Min ED and three different fusion rules at $\gamma = -14$ dB for $2x$ -oversampled PU signal, the channel model is SUI-I with frequency flat lognormal fading with standard deviation 9 dB, the number of sensing stations $M = 8$, the length of FFT $N_{FFT} = 8$, the sample complexity $N = 10240$, and 0.1 dB noise uncertainty.

5.5 Chapter Summary

In this chapter, novel cooperative Max-Min ED based sensing algorithms were presented. The proposed novel technique is robust to noise uncertainty. The chapter presented three different approaches: Max-Min ED, differential Max-Min ED, and Maximum/Minimum ED based CSS. Max-Min ED outperformed the other approaches under various conditions, like no oversampling, small oversampling, and $2x$ -oversampling. Compared to the advanced spectrum sensing techniques which are immune to the noise uncertainty effect, like eigenvalue based methods, the proposed Max-Min ED has significantly reduced complexity.

The basic idea behind the proposed Max-Min ED is to use the frequency variability of SED outputs and to determine the maximum and minimum statistics. Maximum and minimum statistics are utilized to construct the decision statistics. Detection and false alarm probabilities are calculated according to the present and absent hypothesis by comparing predetermined threshold to the decision statistics. Cooperation among a number of sens-

ing stations were exploited with different linear fusion rules. CSS with different fusion rules were presented as a solution to the practical wireless channel issues like hidden node problem. Additionally, analytical results were presented and compared to the simulation result and they were found to match very well.

6. CONCLUSION

This study principally focused on the spectrum sensing function in the CR systems. The study resulted in better understanding and handling of ED based semi-blind spectrum sensing approaches. Specifically, the study focused on the subband based CSS methods. Additionally, the studies have covered the traditional ED based cooperative techniques, FFT/AFB based cooperative method, and Max-Min ED based novel cooperative techniques. These contributions are shortly summarized below.

Chapter 3 covered the collaborative approach exploited between CR receivers to counteract the practical wireless channel effects. Detection performance was enhanced with the collaboration among the CR receivers. Linear fusion rules were implemented to combine the decisions from the individual CR receivers. Reliability of the spectrum sensing increased with the involvement of more CR receivers and the hidden node problem was eliminated. Different fusion rule performance was investigated and "Majority rule" with moderate metrics i.e., P_D and P_{FA} was found to be the best rule. Cooperation was employed that enabled the sensing algorithms to detect the PU signals even at low SNR level.

Chapter 4 contributed on better understanding of subband based spectrum sensing approaches and proposed FFT/AFB based CSS method. Studies considered wideband spectrum sensing that divided the received signal into a number of subband and each subband was processed based of ED algorithms. Subband based spectrum sensing ensured the smallest sensing time and increased detection performances for the wideband signal. For subband based studies, 802.11g standard OFDM based WLAN and 802.11g like FBMC based WLAN were considered. With better spectral containment, FBMC showed the best performances. In these studies, a spectral hole in between two multicarrier was under sensing. The width of the spectral holes was determined to find out the possibility of SU communication. AFB processing of FBMC signal showed significant enhancement, i.e., lowest false alarm probabilities.

Chapter 5 contributed on understanding and handling of a novel maximum-minimum based CSS method. The study proposed novel cooperative Max-Min ED which is immune to noise uncertainty effect and reduces the implementation complexity. The proposed spectrum sensing method that utilizes the frequency variability of SED. Maximum and minimum statistics were used to decide the presence or absence of PU signals with the help of predefined threshold. The Max-Min ED approach removes the noise floor from the

signal that is additive in nature, which makes the algorithm stable to the noise uncertainty effects. Numerical results were presented in these studies. The proposed algorithm has reduced complexity compared to the eigenvalue based approach. The proposed method exhibited around 10 dB sensitivity enhancement for 1 dB noise uncertainty condition in contrast to the traditional cooperative ED. Analytical performance analysis was presented for the proposed algorithm and it matched well with the simulation results.

The overall contributions of the thesis can be summarized as better understanding and handling of CSS in CR system. The proposed novel cooperative Max-Min ED is simple to implement and immune to the noise uncertainty effects. Contributions of these studies are expected to provide useful tools for the design and implementation of simple, flexible and efficient spectrum sensing mechanisms.

REFERENCES

- [1] Federal Communications Commission (FCC), "Spectrum policy task force," Rep. ET Docket no. 02-135, Nov. 2002.
- [2] M. McHenry, "Frequency agile spectrum access technologies," in FCC Workshop on Cognitive Radio, Washington US, May 2003.
- [3] S. Haykin, "Cognitive radio: Brain-empowered wireless communications," *IEEE Journal on Selected Areas Communications*, vol. 23, no. 2, pp. 201-220, Feb. 2005.
- [4] A. Mariani, A. Giorgetti, M. Chiani, "Recent advances on wideband spectrum sensing for cognitive radio," in *Cognitive communication and cooperative HetNet coexistence*, Switzerland: Springer International Publishing, pp 1-31, Jan. 2014.
- [5] G. Staple and K. Werbach, "The end of spectrum scarcity," *IEEE Spectrum*, vol. 41, no. 3, pp. 48-52, Mar. 2004.
- [6] T. Yucek and H. Arslan, "A Survey of spectrum sensing algorithms for cognitive radio applications," in *IEEE Communications Surveys and Tutorials*, vol. 11, no. 1, pp. 116-129, first quarter 2009.
- [7] J. Mitola and G. Q. Maguire, "Cognitive radio: making software radios more personal," in *IEEE Personal Communications*, vol. 6, pp. 13-18, Aug. 1999.
- [8] H. Poor, *An introduction to signal detection and estimation*, New York, NY: Springer New York, 1994.
- [9] S. Kandeepan, A. Giorgetti, "Spectrum sensing in cognitive radio," in *Cognitive radios and enabling techniques*, Artech House Publishers, Boston, 2012.
- [10] H. Urkowitz, "Energy detection of unknown deterministic signals," in *Proc, IEEE*, vol. 55, no. 4, pp. 523-531, Apr. 1967.
- [11] G. Ganesan and Y. Li, "Cooperative spectrum sensing in cognitive radio, part I: two user networks," in *IEEE Transactions on Wireless Communications*, vol. 6, no. 6, pp. 2204-2212, June 2007.
- [12] G. Ganesan and Y. (Geoffrey) Li, "Cooperative spectrum sensing in cognitive radio, part II: multiuser networks," in *IEEE Transactions on Wireless Communications*, vol. 6, no. 6, pp. 2214-2222, June 2007.
- [13] C. You, H. Kwon, and J. Heo, "Cooperative TV spectrum sensing in cognitive radio for Wi-Fi networks," in *IEEE Transactions on Consumer Electronics*, vol. 57, no. 1, pp. 62-67, Feb. 2011.

- [14] S. Atapattu, C. Tellambura and H. Jiang, "Energy detection based cooperative spectrum sensing in cognitive radio networks," in *IEEE Transactions on Wireless Communications*, vol. 10, no. 4, pp. 1232-1241, April 2011.
- [15] S. Dikmese, "Enhanced spectrum sensing techniques for cognitive radio," Ph.D. dissertation, Tampere University of Technology, Tampere, Finland, March 2015.
- [16] Z. Zheng, "Experimental evaluation of spectrum sensing," M.S. thesis, Tampere University of Technology, Tampere, Finland, May 2014.
- [17] S. Dikmese, M. Renfors and H. Dincer, "FFT and filter bank based spectrum sensing for WLAN signals," in *Proc. ECCTD'11 conf.*, Linköping, Sweden, August 2011.
- [18] P. Cheraghi, Y. Ma, Z. Lu, and R. Tafazolli, "A novel low complexity differential energy detection for sensing OFDM sources in low SNR environment," in *IEEE GLOBECOM Workshops*, pp. 378-382, Dec. 2011.
- [19] Y. Zeng, Y.-C. Liang, A. T. Hoang, and R. Zhang, "A Review on spectrum sensing for cognitive radio: challenges and solutions," in *EURASIP Journal on Advances in Signal Processing*, vol. 2010, pp. 1-16, Jan. 2010.
- [20] S. Haykin, "Cognitive radio" in *Cognitive dynamic systems*, Cambridge, UK, Cambridge University Press, ch. 7, pp. 230-276, 2012.
- [21] M. S. Hossain, M. I. Abdullah, "Hard decision based cooperative spectrum sensing over different fading channel in cognitive radio," in *International Journal of Economics & Management Sciences*, vol. 1, no. 1, pp. 84-93, Nov. 2012.
- [22] S. Althunibat, M. Di Renzo, and F. Granelli, "Optimizing the K-out-of-N rule for cooperative spectrum sensing in cognitive radio networks," in *IEEE GLOBECOM'13*, pp. 1607-1611, Dec. 2013.
- [23] R. Qiu, Z. Hu and H. Li, "OFDM cognitive radio network" in *Cognitive radio communication and networking*. Chichester, West Sussex, UK: Wiley-Blackwell, ch. 9, sec. 9, pp. 339-350, 2012.
- [24] G. Bansal, J. Hossain, and V. K. Bhargava, IEEE, "Adaptive power loading for OFDM-Based cognitive radio systems with statistical interference constraint," in *IEEE Transactions on Wireless Communications*, vol. 10, no. 9, pp. 2786-2791, Sep. 2011.
- [25] Y. Cui, Z. Zhao, and H. Zhang, "An efficient filter banks based multicarrier system in cognitive radio networks," in *Radioengineering*, vol. 19, no. 4, pp. 479-487, Dec. 2010.

- [26] S. Dikmese and M. Renfors, "Performance analysis of eigenvalue based spectrum sensing under frequency selective channels," in Proc. CROWNCOM'12, Stockholm, Sweden, pp. 356-361, June 2012.
- [27] S. Dikmese, A. Gokceoglu, M. Valkama and M. Renfors, "Reduced complexity spectrum sensing based on maximum eigenvalue and energy," in Proc. ISWCS'13, Ilmenau, Germany, Aug. 2013.
- [28] S. Dikmese, J. L. Wong, A. Gokceoglu, E. Guzzon, M. Valkama and M. Renfors, "Reducing computational complexity of eigenvalue based spectrum sensing for cognitive radio," in Proc. CROWNCOM'13, Washington DC, USA, pp. 61-67, July 2013.
- [29] S. Dikmese, P.C. Sofotasios, M. Renfors, M. Valkama and M. Ghogho, "Analysis and mitigation of noise uncertainty and frequency selectivity effects in wide-band multimode sensing methods for cognitive radio," accepted to IEEE GLOBECOM'15 conf., San Diego, USA, Dec. 2015.
- [30] R. Jain, "Channel models: A tutorial," in WiMAX Forum AATG, pp. 1-6, 2007.
- [31] S. Dikmese and M. Renfors, "Optimized FFT and filter bank based spectrum sensing for bluetooth signal," in Proc. WCNC'12 conf., Paris, France, April 2012.
- [32] S. Dikmese, S. Srinivasan and M. Renfors, "FFT and filter bank based spectrum sensing and spectrum utilization for cognitive radios," in Proc. 5th International Symposium on Communications, Control and Signal Processing, Rome, Italy, pp 1-5, May 2012.
- [33] S. Srinivasan, S. Dikmese and M. Renfors; "Spectrum sensing and spectrum utilization model for OFDM and FBMC based cognitive radios," in Proc. SPAWC'12 conf. Izmir, Turkey, June 2012.
- [34] S. Dikmese, T. Ihalainen and M. Renfors, "Analysis and optimization of energy detection for non-flat spectral characteristic," book chapter in cognitive communication and cooperative HetNet coexistence, Signal and Communication Technology Series, in Springer, pp.47-69, Jan. 2014.
- [35] S. Dikmese, S. Srinivasan, M. Shaat, F. Bader and M. Renfors, "Spectrum sensing and spectrum allocation for multicarrier cognitive radios under interference and power constraints," in EURASIP Journal on Advances in Signal Processing, 2014:68, DOI: 10.1186/1687-6180-2014-68, May 2014.

- [36] S. Dikmese, A. Loulou, S. Srinivasan and M. Renfors, "Spectrum sensing and resource allocation models for enhanced OFDM based cognitive radio," in Proc. CROWNCOM'14 conf., Oulu, Finland, June 2014.
- [37] S. Dikmese, P. C. Sofotasios, T. Ihalainen, M. Renfors and M. Valkama "Efficient energy detection methods for spectrum sensing under non-flat spectral characteristics," in IEEE Journal on Selected Areas in Communications, vol.33, issue.5, 755-770, May 2015.
- [38] S. Dikmese, P.C. Sofotasios, M. Renfors and M. Valkama, "Subband energy based reduced complexity spectrum sensing under noise uncertainty and frequency-selective spectral characteristics," in IEEE Transaction on Signal Processing, DOI:10.1109/TSP.2015.2480048, Sep. 2015.
- [39] S. Dikmese, Z. Zheng, P.C. Sofotasios, M. Renfors and M. Valkama, "Efficient wireless microphone sensing: Subband energy detector principle and measured performance," in Proc. IEEE ICC'15., London, UK, June 2015.
- [40] S. Dikmese, P.C. Sofotasios, M. Renfors and M. Valkama, "Maximum-minimum energy based spectrum sensing under frequency selectivity for cognitive radios," in Proc. CROWNCOM'14 conf., Oulu, Finland June 2014.